

SOIL-WATER CHARACTERIZATION AND UNSATURATED
SHEAR STRENGTH OF KHON KAEN LOESS

Miss Maria Emilia Pambid Sevilla

A Thesis Submitted in Partial Fulfillment of the Requirements
for the Degree of Master of Engineering Program in Civil Engineering
Department of Civil Engineering
Faculty of Engineering
Chulalongkorn University
Academic Year 2013

Copyright of Chulalongkorn University

บทคัดย่อและแฟ้มข้อมูลฉบับเต็มของวิทยานิพนธ์ตั้งแต่ปีการศึกษา 2554 ที่ให้บริการในคลังปัญญาจุฬาฯ (CUIR)

เป็นแฟ้มข้อมูลของนิสิตเจ้าของวิทยานิพนธ์ที่ส่งผ่านทางบัณฑิตวิทยาลัย

The abstract and full text of theses from the academic year 2011 in Chulalongkorn University Intellectual Repository (CUIR)
are the thesis authors' files submitted through the Graduate School.

คุณลักษณะเฉพาะระหว่างดินกับน้ำและกำลังรับแรงเฉือนแบบไม่อิ่มตัวด้วยน้ำ

ของดินลมหอบ จ.ขอนแก่น

นางสาว มาเรีย อิมิลล่า พามบิต เซวิลล่า

วิทยานิพนธ์นี้เป็นส่วนหนึ่งของการศึกษาตามหลักสูตรปริญญาวิศวกรรมศาสตรมหาบัณฑิต

สาขาวิชาวิศวกรรมโยธา ภาควิชาวิศวกรรมโยธา

คณะวิศวกรรมศาสตร์ จุฬาลงกรณ์มหาวิทยาลัย

ปีการศึกษา 2556

ลิขสิทธิ์ของจุฬาลงกรณ์มหาวิทยาลัย

Thesis Title	Soil-Water Characterization and Unsaturated Shear Strength of Khon Kaen Loess
By	Miss Maria Emilia Pambid Sevilla
Field of Study	Civil Engineering
Thesis Advisor	Associate Professor Suched Likitlersuang, D.Phil.

Accepted by the Faculty of Engineering, Chulalongkorn University in Partial
Fulfillment of the Requirements for the Master's Degree

.....Dean of the Faculty of Engineering
(Associate Professor Boonsom Lerthirunwong, Dr.Ing.)

THESIS COMMITTEE

.....Chairman
(Associate Professor Supot Teachavorasinskun, D.Eng.)

..... Thesis Advisor
(Associate Professor Suched Likitlersuang, D.Phil.)

..... Examiner
(Associate Professor Tirawat Boonyatee, D.Eng.)

..... External Examiner
(Associate Professor Watcharin Gasaluck, Ph.D.)

มาเรีย อิมิลล่า พามบิต เซวิลล่า : คุณลักษณะเฉพาะระหว่างดินกับน้ำและกำลังรับแรง
 เชื้อแบบไม่อิ่มตัวด้วยน้ำของดินลมหอบ จ.ขอนแก่น. (SOIL-WATER
 CHARACTERIZATION AND UNSATURATED SHEAR STRENGTH OF KHON
 KAEN LOESS) อ.ที่ปรึกษาวิทยานิพนธ์หลัก : รศ.ดร.สุเชษฐ ลิขิตเลอสรวง, 77 หน้า.

ดินลมหอบขอนแก่นเป็นดินชนิดวิบัติเมื่ออยู่ในสภาวะชุ่มน้ำ ซึ่งเป็นสาเหตุให้เกิดความ
 อันตรายและเสียหายแบบฉับพลันต่อสิ่งก่อสร้างได้ ดินประเภทนี้สามารถอธิบายพฤติกรรมได้
 ด้วยเส้นโค้งลักษณะเฉพาะระหว่างดินกับน้ำ ซึ่งคือความสัมพันธ์ระหว่างปริมาณน้ำเชิงปริมาตร
 กับเมตริกซ์คูดน้ำ งานวิจัยนี้ศึกษาพฤติกรรมแบบไม่อิ่มตัวด้วยน้ำของดินลมหอบขอนแก่นใน
 ห้องปฏิบัติการด้วยเครื่องมือแรงอัดสามแกนแบบไม่อิ่มตัวด้วยน้ำ แบบจำลองของแวนเกนนู
 เซน และแบบจำลองเฟรดริ้นและซิง ถูกนำมาใช้จำลองเส้นโค้งลักษณะเฉพาะระหว่างดินกับน้ำ
 ส่วนแบบจำลองมอร์คลอมม์แบบขยายความได้ถูกนำมาใช้อธิบายพฤติกรรมด้านกำลังของดิน
 ไม่อิ่มตัวด้วยน้ำ นอกเหนือจากนี้งานวิจัยยังได้ใช้ข้อมูลผลการทดสอบจากการศึกษาในอดีตที่
 มหาวิทยาลัยขอนแก่นร่วมในการวิเคราะห์ด้วย งานวิจัยพบว่าแบบจำลองเฟรดริ้นและซิงเหมาะ
 สำหรับการจำลองเส้นโค้งลักษณะเฉพาะระหว่างดินกับน้ำของดินลมหอบขอนแก่น
 นอกเหนือจากนี้ จากการวิเคราะห์ผลการทดสอบด้วยระเบียบวิธีทางสถิติสามารถกำหนด
 ค่าพารามิเตอร์สำหรับแบบจำลองมอร์คลอมม์แบบขยายความได้อีกด้วย

ภาควิชา.....วิศวกรรมโยธา..... ลายมือชื่อนิติ.....
 สาขาวิชา.....วิศวกรรมโยธา..... ลายมือชื่อ อ.ที่ปรึกษาวิทยานิพนธ์หลัก.....
 ปีการศึกษา..... 2556.....

5470516821: MAJOR CIVIL ENGINEERING

KEYWORDS: SOIL-WATER CHARACTERISTIC CURVE/ UNSATURATED SOIL/ SHEAR STRENGTH/ LOESS/ KHON KAEN

MARIA EMILIA PAMBID SEVILLA: SOIL-WATER CHARACTERIZATION AND UNSATURATED SHEAR STRENGTH OF KHON KAEN. ADVISOR: ASSOC. PROF. SUCHED LIKITLERSUANG, D.Phil., 77 pp.

Khon Kaen Loess, being known as a collapsible soil, could cause hazards such as sudden collapse and settlement when subjected to wetting. This soil could be further examined with the use of soil-water characteristic curve – the relationship between the volumetric water content and the matric suction. This research presents an experimental study of unsaturated behavior of Khon Kaen Loess by means of the unsaturated triaxial apparatus. The soil-water characteristic curves were modelled using the curve fitting equations of Van Genuchten (1980) and Fredlund and Xing (1994). Additionally, the shear strength of unsaturated soil was explained using an extended Mohr-Coulomb failure criterion, which is fitted to the unsaturated shear strength equation by Fredlund *et al.* (1978). The research also employed the testing data of Khon Kaen Loess from previous study at Khon Kaen University. The research findings determined that the Fredlund and Xing (1994) model best fits for the soil-water characteristic curve of Khon Kaen Loess. The data analysis of the unsaturated shear strength shows that from the extended Mohr-Coulomb parameter values for Khon Kaen Loess could be derived.

Department: Civil Engineering Student's Signature

Field of Study: Civil Engineering Advisor's Signature

Academic Year: 2013

ACKNOWLEDGEMENTS

I would like to sincerely thank The Lord. For without him nothing is possible, and with Him, anything is possible.

AUN/Seed-Net, for granting me this scholarship. Providing us what we need and giving us the chance to meet another culture, another country, and another hope.

My thesis adviser, Ajarn Suched. For enthusiastically sharing his knowledge, supporting and encouraging me at all times.

P' Pik and Jem, who helped me, carry all the burden of testing, who have been patient and helpful in every step of the way. Hai Yen who kept my dark days bright, my friend and family, who had and has always been there for me. To keep getting better. To fight harder.

My family and friends back home, for they were my inspiration to go forward and live life.

My panel, Ajarn Watcharin of Khon Kaen University, for the continuous support and extensive effort imparted in this research.

Finally, I would like to thank my committee, Assoc. Prof. Dr. Supot Teachavorasinskun and Assoc. Prof. Dr. Tirawat Boonyatee.

Contents

	Page
Abstract (Thai)	iv
Abstract (English)	v
Acknowledgements	vi
Contents	vii
List of Tables	x
List of Figures	xi
CHAPTER I INTRODUCTION	1
1.1 Background of the study	1
1.2 Objectives	2
1.3 Scope of the study	2
1.4 Assumptions	3
CHAPTER II LITERATURE REVIEW	4
2.1 Unsaturated Soil Mechanics	4
2.1.1 Four Phase State of Unsaturated Soil	5
2.1.2 Capillary Model	6
2.1.3 Hysteresis	10
2.1.4 Soil Suction	11
2.2 Soil-Water Characteristic Curve	12
2.2.1 Typical Components and Shape	13
2.2.2 Fredlund and Xing with correction factor (1994)	15
2.2.3 Van Genuchten (1980)	16
2.3 Instrumentation and Measurement	17
2.3.1 Pressure Plate Extractor (0 to 1500 kPa)	18
2.3.2 Tensiometers (0 to 100 kPa)	19
2.3.3 Hanging Column (0 to 100 kPa)	20

	Page
2.3.4 Filter Paper (Entire Range of Suction).....	21
2.3.5 Unified measurement system with suction control	22
2.4 Unsaturated Shear Strength Criteria	23
2.5 Existing works	24
2.6 Multiple Regression	26
2.6.1 Least Square Estimation of the Parameters	26
2.6.2 Hypothesis Testing in Multiple Linear regression.....	27
2.6.3 R-squared	27
CHAPTER III METHODOLOGY	28
3.1 Materials	28
3.1.1 Preparation of Sample for testing	29
3.2 Instrumentation	29
3.3 Triaxial Stages	34
3.3.1 Saturation	34
3.3.2 Isotropic Consolidation	34
3.3.3 Soil-Water Curve Stage	35
3.4 SWCC Construction.....	35
3.5 Shear Strength Analysis.....	36
CHAPTER IV RESULTS AND DISCUSSIONS	37
4.1 Review of Fitting equations	37
4.2 Calibration of Unsaturated Triaxial Test with standard sand	38
4.2.1 Toyoura and Ottawa sand	38
4.2.2 Designation of Tested Sands.....	39
4.2.3 Results of SWCC	40
4.2.4 Fitted Models	41
4.2.5 Discussion of results	44
4.3 SWCC of Khon Kaen Loess	46
4.3.1 Soil properties	46
4.3.2 Matric suction from Unsaturated Triaxial Testing.....	47
4.3.3 Model Fitting for a net confining pressure of 150 kPa	48

	Page
4.3.4 Model Fitting for a net confining pressure of 200 kPa	50
4.3.5 Comparison with existing models.....	53
4.3.6 Unified Khon Kaen SWCC.....	54
4.4 Analysis of Khon Kaen Data	57
4.4.1 Unsaturated shear strength.....	61
4.4.2 Fitted model and unsaturated parameters	62
4.5 Comparison with existing works	62
4.6 Shear testing under triaxial conditions.....	63
4.5.1 Unconsolidated Undrained Test.....	63
4.5.2 Consolidated Undrained Test.....	67
CHAPTER V CONCLUSION AND RECOMMENDATION.....	70
5.1 Conclusion	70
5.2 Recommendations.....	71
REFERENCES.....	72
APPENDIX.....	75
BIOGRAPHY	77

List of Tables

	Page
Table 2.1: Summary of suction measurement methods	17
Table 2.2: Multiple Regression Data Lay-out (Montgomery, 2003)	26
Table 4.1: Properties of tested sands.....	39
Table 4.2: Designation of Tested Sands	39
Table 4.3: Minimizing Sum of Square Error for Fredlund and Xing (1994) model....	41
Table 4.4: Minimizing Sum of Square Error for Van Genuthcen (1980) model	42
Table 4.5: Summary of fitting parameters for Toyoura Sand	43
Table 4.6: Results of <i>t-test</i> for Toyoura Sand	44
Table 4.7: Index Properties of Red Khon Kaen Loess.....	46
Table 4.8: Minimizing Sum of Square Error for Fredlund and Xing (1994) model....	48
Table 4.9: Minimizing Sum of Square Error for Van Genuchten (1980) model	48
Table 4.10 Result of <i>t-test</i> for 150 kPa net confining stress test.....	48
Table 4.11: Summary of fitting parameters under a net stress of 150 kPa	50
Table 4.12: Minimizing Sum of Square Error for Fredlund and Xing (1994) model..	50
Table 4.13: Minimizing Sum of Square Error for Van Genuchten (1980) model	50
Table 4.14 Result of <i>t-test</i> for 200 kPa net confining stress test.....	51
Table 4.15: Summary of fitting parameters under a net stress of 200 kPa	52
Table 4.16: Prediction of Median SWCC using Fredlund and Xing (1994)	55
Table 4.17 Prediction of Median SWCC using Van Genuchten (1980).....	55
Table 4.18: Summary of fitting parameters for the median SWCC	56
Table 4.19: Khon Kaen properties and parameters.....	58
Table 4.20: Regression Statistics	61
Table 4.21: Analysis of Variance.....	61
Table 4.22: Coefficient table.....	61

List of Figures

	Page
Figure 1.1: Deposit of Loess in Thailand (Phien-wej, 1992).....	1
Figure 2.1: Categorization of soil mechanics based on engineering applications (Fredlund, 1996).....	2
Figure 2.2: Physical model and phenomenon related to capillarity (Fredlund and Rajardo, 1993)	6
Figure 2.3: (a) Inter-molecular forces on contractile skin and water; (b) pressures and surface tension acting on a curved two-dimensional surface (Ng and Menzies, 2007).....	7
Figure 2.4: Equilibrium of a 3D double-curvature air-water interface (Lu and Likos, 2007)	9
Figure 2.5: Effects of Height and Radius to Capillarity. (Fredlund, 1993)	10
Figure 2.6: Relationship between matric suction, pore radius and capillary height. (Fredlund, 1993)	11
Figure 2.7: Definition of Variables from SWCC (Zhai et.al, 2012)	13
Figure 2.8: Typical Curves of SWCC (Lu and Likos, 2004).....	14
Figure 2.9: Sample plot for the effect of n parameter (Fredlund and Xing, 1994).....	15
Figure 2.10: Sample plot for the effect of n parameter (Fredlund and Xing, 1994)....	16
Figure 2.11: Pressure plate extractor system. (Indrawan, 2006).....	18
Figure 2.12: Common types of Tensiometer configurations (a) Manometer type (b) Gauge type (c) Transducer type (Ng et.al, 2007)	19
Figure 2.13: Schematic Diagram of a Hanging Column Apparatus (ASTM D 6836: 02).....	20
Figure 2.14: Contact and noncontact filter paper methods for measuring matric and total suction, respectively. (Fredlund, 1993)	21
Figure 2.15: Calibration curves for two types of filter paper. (Fredlund, 1993)	21
Figure 2.16: Unified measurement system with suction control (Rouf, et. al., 2012) ..	22

	Page
Figure 2.17: Extended shear strength for unsaturated soils (Fredlund, 1993).....	23
Figure 2.18: SWCC of compacted khon kaen loess by hanging column, pressure plate and isopiestic humidity method (Nuntasarn, 2011)	25
Figure 2.19: SWCC of Khon Kaen loess by Pressure plate method and Vapour equilibrium technique (Punrattanasin et. al, 2002)	25
Figure 3.1: Soil Sampling. (a) The response of shredding of the soil due to evaporation in the topsoil layer and (b) shows the test pit at 2.50m. to 3.00 m at Khon Kaen University (c) the fragility of the soil sample (d) manual block sampling done.	28
Figure 3.2: The unsaturated triaxial system set-up	30
Figure 3.3: The triaxial cell diagram with air and water connections (Wykeham Farrance, 2010).....	31
Figure 3.4: Air Pressure Controller.....	32
Figure 3.5: Hydromatic Pressure Controllers	32
Figure 3.6: Automatic Volume Change Devices	32
Figure 3.7: Pressure panel.....	32
Figure 4.1: Grain Size Distribution of Tested Sands	38
Figure 4.2: Raw test results for sand.....	40
Figure 4.3: Modelling with FX and VG.....	43
Figure 4.4: Suction values compared with existing work.....	45
Figure 4.5: Grain Size Distribution of tested soil	46
Figure 4.6: Plot of volumetric water content and suction of Khon Kaen Loess under a net confining stress of 150 kPa and 200 kPa.....	47
Figure 4.7: SWCC of Khon Kaen Loess under 150 kPa net stress.....	49
Figure 4.8: SWCC of Khon Kaen Loess under 200 kPa net stress.....	52
Figure 4.9: SWCC comparisons with existing works.....	53
Figure 4.10: Average curve for tested and fitted	54
Figure 4.11: Khon Kaen SWCC	57

	Page
Figure 4.12: Unsaturated shear strength plane.....	62
Figure 4.13: Sample after UU test	64
Figure 4.14: Comparison of sheared sample with the original size.....	65
Figure 4.15: Shear path along the s' and t in UU testing.....	65
Figure 4.16: Shear path of p' and q in UU testing.....	66
Figure 4.17 Axial Strain vs. Deviator Stress.....	66
Figure 4.18: Shear failure on a CU test.....	67
Figure 4.19 Axial Strain vs. Deviator Stress in a CU test.....	68
Figure 4.20 Stress path of s' vs t in a CU test	68
Figure 4.21 Shear path of p' vs q in a CU test	69

CHAPTER I

INTRODUCTION

1.1 Background of the study

A problematic collapsible soil in the form of Loess is abundant in the North-Eastern part of Thailand as illustrated in Figure 1.1. It has been known to possess remarkable strength in its natural state but rapid collapse is experienced when imbibition in the soil occurs (Phien-wej et.al, 1992). To better illustrate the series, unsaturated soil mechanics was called upon to assess the strength behavior of the soil in terms of the change in soil suction corresponding a change in volumetric water content.



Figure 1.1: Deposit of Loess in Thailand (Phien-wej, 1992)

Studies in the past two decades have been dedicated to be able to better grasp the behavior of this soil with the use of soil-water characteristic curve or SWCC,

which is a non-linear relationship of the water content and suction. Further analysis may be derived from this relationship such as hydraulic conductivity, water storage functions and shear strength. Although it has proven essential to the implementation of unsaturated soil mechanics in the context of geotechnical engineering (Fredlund, 2000), careful consideration must be made.

1.2 Objectives

The primary objective of the study is to conduct an experimental research of unsaturated soil and analyze its subsequent relationship with regards to matric suction, volumetric water content and shear strength. This will be accomplished by performing unsaturated triaxial testing.

In order to describe the behavior of the soil and establish a simple and better understanding of the concept, the unsaturated shear strength parameters will be analyzed with the aid of statistics.

1.3 Scope of the study

The study limits itself to the following criteria:

1. The unsaturated triaxial testing was performed on undisturbed samples from Khon Kaen soil, obtained from the North-East of Thailand.
2. The test procedures and results are also limited to the capabilities of unsaturated triaxial system.
3. The effect of temperature of the soil particles, air and water in the soil matrix are considered irrelevant to the suction.
4. SWCC was modelled on two mathematical models which are: Van Genuchten (1980) and Fredlund & Xing (1994).

1.4 Assumptions

The following assumptions should be considered:

1. Soil specimen is assumed to be *undisturbed* during the time of sampling.
2. No evaporation or addition of water content occurred during the sampling and transportation of the specimen from the site to the laboratory.
3. All testing equipment is properly calibrated at the time of experimentation.
4. The pore pressures and stress distributions are equal throughout the specimen.
5. All gathered data from literature are correct and unbiased.

CHAPTER II

LITERATURE REVIEW

In this chapter, knowledge related to unsaturated soil mechanics are introduced to give some general overview of the analysis. Then, the different testing methods to obtain the SWCC are discussed and finally statistical analysis is presented.

2.1 Unsaturated Soil Mechanics

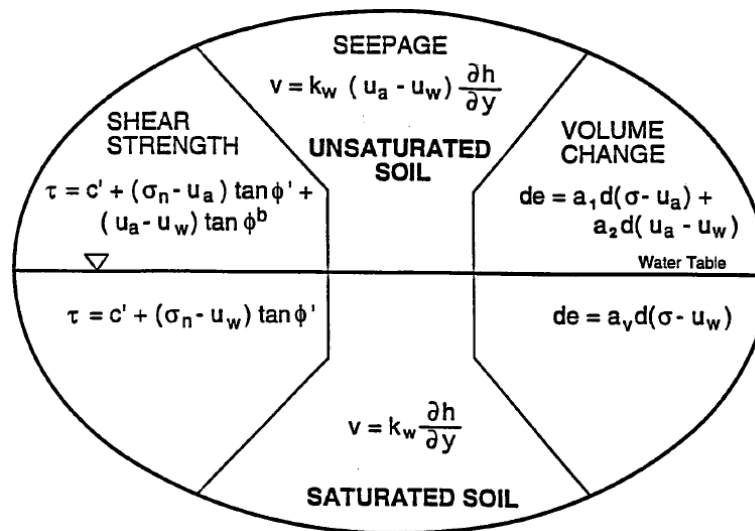


Figure 2.1: Categorization of soil mechanics based on engineering applications (Fredlund, 1996)

Pioneers of unsaturated soil mechanics called upon that certain geotechnical engineering problems may be analyzed with more knowledge and understanding of the unsaturated soil behavior. Identification of the primary needs and difficulties in the discipline which needs to be addressed were stated as follows (Fredlund and Rajardo, 1993):

- a. Negative pore-water pressure measurement which may either be direct or indirect.
- b. Integration of SWCC information. It is important to collect data for diverse kinds of soils.

- c. Simplification of formulas for distinct and various unsaturated soil problems.
- d. Documentation of case histories involving unsaturated soil behavior.

Mairaing et. al (2011) called upon pertinent application of suitable technology for unsaturated soil mechanics such as rainfall-induced landslide, dam engineering and other volume change problems in Thailand. The paper called upon further adaptive study and application of Unsaturated Soil Mechanics not only in Thailand but also for South-East Asian countries; to provide cost-effective and appropriate technology to achieve a better understanding of the subject matter in their own respective circumstances.

It was noted that remarkable and extensive research has been produced in the past decades, but has been futile to draw attention in practical application. It was argued by Blight (2008) that the case is often due to the lack of advancement in new technology and concepts, as well as practical application and evaluation.

2.1.1 Four Phase State of Unsaturated Soil

Partially saturated soil can be brought about by natural and man-made movement. In natural conditions, it is generated when the net surface flux is yielded from the evaporation exceeding the precipitation while man-made activities such as quarrying, remolding and recompaction renders exchange of air and water between the soil and the atmosphere, producing partial saturation.

This assumption of fully saturated and dry conditions may not be appropriate in some applications, such as in evaluating the heave of foundations on swelling or expansive soils (Lu and Likos 2004, Fredlund, et. al. 1993). This common approach in soil mechanics also ignores the presence of the air-water surface that is referred to as the contractile skin; this property is unique to unsaturated soils as it provides the ability to exert a tensile pull called surface tension. In a continuous air phase where

the soil particles are able to interact with the contractile skin, the mechanical behavior of the soil is said to be affected.

Surface tension is a product of the inter-molecular forces which vary from those that behave in the internal water which enables the contractile skin to behave similar to an elastic membrane. It is said to be measured in force per unit length and is tangential to the surface of the contractile skin, moreover the magnitude is inversely proportional to the temperature.

2.1.2 Capillary Model

The major factors that have strong direct effects on the SWCC are the radius of curvature as well as the height of water rise in soil which are apparent consequences of capillary action. The two factors have been established to be inversely proportional.

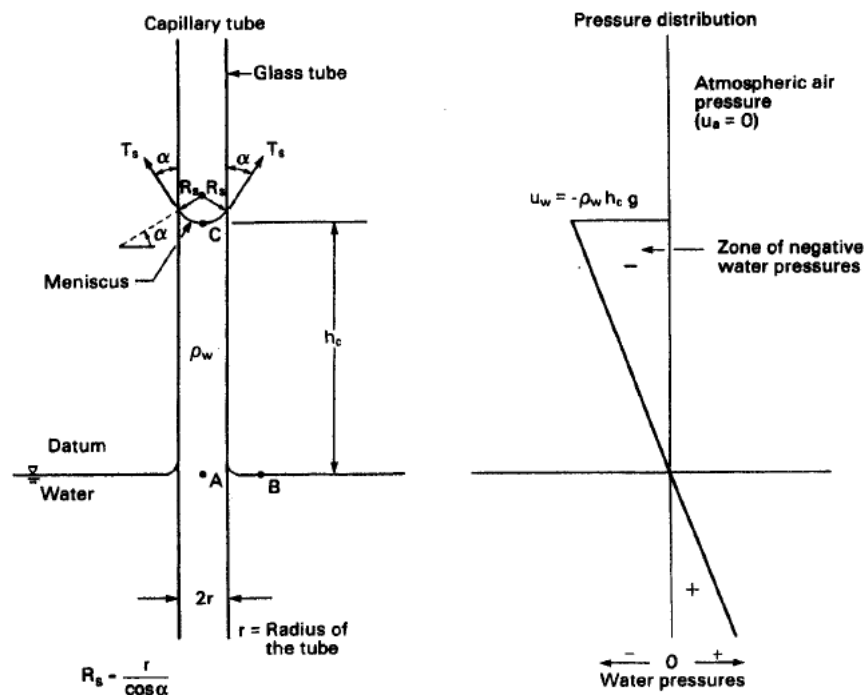


Figure 2.2: Physical model and phenomenon related to capillarity (Fredlund and Rajardo, 1993)

Provided an atmospheric condition, a small-diameter tube introduced into water as shown in Figure 2.2, the surface tension together with the tendency of water to wet the tube surface will cause the water to rise up the tube. This can be analyzed as we consider the surface tension, T_s , that acts at an angle α from the vertical, about the meniscus circumference. This angle is identified as the contact angle and the magnitude is dependent on the adhesion involving the tube material and the molecules of the contractile skin. Consider the vertical force equilibrium of the capillary water in Figure 2.2. We will have equation (1) in the explanation of tension force that is accountable for holding the water up.

$$2 \pi r T_s \cos \alpha = \pi r^2 h_c \rho_w g \quad (1)$$

Simplifying the equation above with assumption that the degree of contact between clean glass and pure water is 0° , the equation results to provide the maximum

water height, $h_c = \frac{2 T_s}{\rho_w g r} \quad (2)$

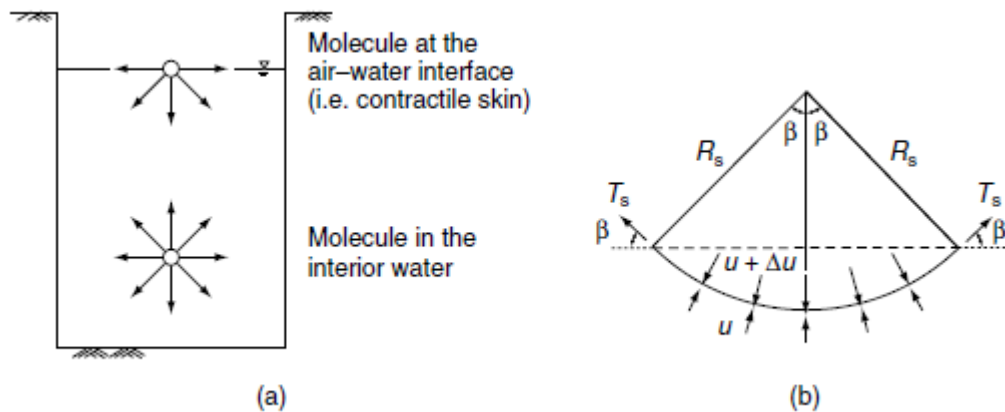


Figure 2.3: (a) Inter-molecular forces on contractile skin and water; (b) pressures and surface tension acting on a curved two-dimensional surface (Ng and Menzies, 2007)

The water molecules from the internal face of the water has balanced forces in all directions as seen in Figure 2.3 (a), however the molecules in the surface experiences instability, producing a curved surface in the direction of the water side.

To be able to establish equilibrium, a tensile force is produced along the contractile skin.

Horizontal forces in the illustration of Figure 2.3 (b) the pressures u , $(u+\Delta u)$ and surface tension, T_s along the radius of curvature of R_s will undertake equilibrium, therefore:

$$2 T_s \sin \theta = 2 \Delta u R_s \sin \theta \quad (3)$$

In a 2D-Surface, the magnitude of $(2 R_s \sin \theta)$ is the horizontal projection of the length of the membrane unto a flat plane. If the equation is simplified, the result will be:

$$\Delta u = \frac{T_s}{R_s} \quad (4)$$

In the case of a 3D-surface, as in Figure 2.4, where R_1 and R_2 are curvature radii of a warped membrane in two perpendicular planes:

$$\Delta u = T_s \left(\frac{1}{R_1} + \frac{1}{R_2} \right) \quad (5)$$

If the radii are equal in every single direction, where $R_1 = R_2 = R_s$, the result will be:

$$\Delta u = \frac{2T_s}{R_s} \quad (6)$$

Matric suction existing in partially saturated soils is subjected to a greater magnitude of air pressure, u_a , compared to the water pressure, u_w . The contractile

skin would therefore conform to the pressure disparity similar to the previous equation.

$$(u_a - u_w) = \frac{2T_s}{R_s} \quad (7)$$

Therefore greater matric suction can be expected from a diminutive curvature radius and as this suction approaches zero, the radius draws to infinity, producing a flat air and water interface. The same way that soil water behaves; the smaller soil pore radius, the greater suction is anticipated.

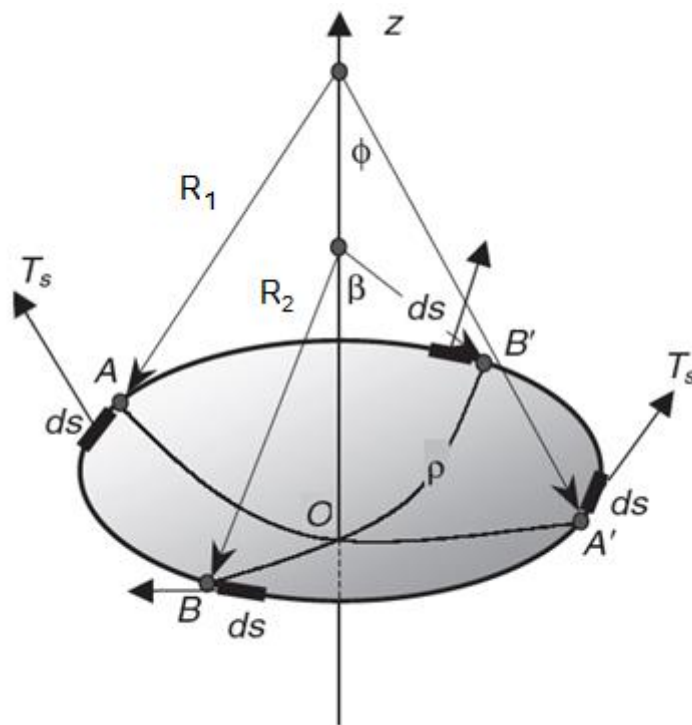


Figure 2.4: Equilibrium of a 3D double-curvature air-water interface (Lu and Likos, 2007)

2.1.3 Hysteresis

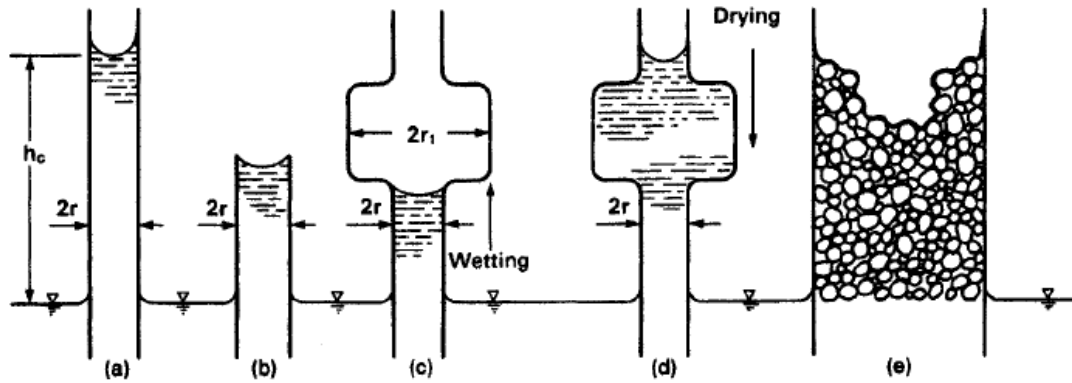


Figure 2.5: Effects of height and radius to capillarity. (Fredlund, 1993)

The full potential of water to rise is given by Figure 2.5 (a); the subsequent, which is (b), illustrates how the height of the tube can limit the escalation thereby increasing the radius if precise abundance of the previous equations is to be strictly observed.

Significance of the radial aperture is exemplified in Figure 2.5 (c), (d) and (e); obstructions of the increase or decrease in h_c are shown. The last illustration exemplifies that the potential capillary height may be attained as long as adequate openings which are still capable of engaging surface tension exist.

Therefore, it is expected that the curves for a single sample are expected to be different for the wetting and drying state. The drying curve which is obtained from an at the outset saturated and then the water is desorbed by suction which approaches the dry state, after which by decreasing the suction, water gradually adjoins the sample and the wetting curve is obtained. The variation between the wetting and drying curve is known as hysteresis whose phenomenon is caused by several factors, one is the geometric effect which is commonly termed as ink-bottle effect. This was illustrated in Figure 2.5. Second is the effect of the contact angle between the water and soil particle which is larger at the time of an advancing water front. This advancing meniscus possesses lower matric suction since it is comprised of a larger radius of

curvature compared to a drying meniscus. Third is that trapped air during the wetting-drying process will eventually become dissolved in the mixture.

The effect of hysteresis may also be accentuated by the shrinking or swelling of expansive soils as well as the rate of shrinking and swelling. (Fetter, 1999)

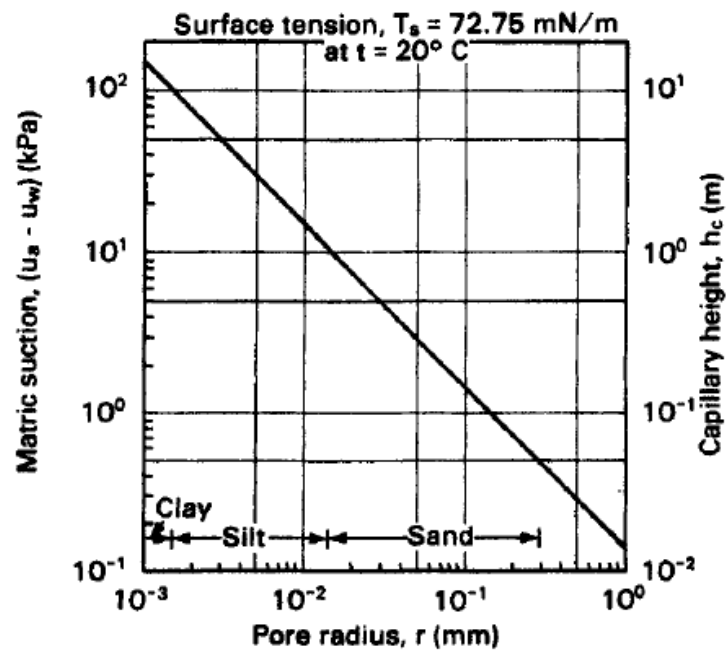


Figure 2.6: Relationship between pore radius, matric suction and capillary height. (Fredlund, 1993)

2.1.4 Soil Suction

During the 1900's, the inception of soil suction science began in the investigation of the soil-plant-water system. In the engineering field, the importance was pioneered by the Road Research Laboratory in England with regards to pertinence in the unsaturated soil mechanical behavior

In the study of geotechnical engineering, potential energy is the primary concern. It is the sum of the partial constituents driven by matric, osmotic, pressure and gravitational potentials. (Nam S. et. al., 2009)

$$T = M + O + P + z \quad (8)$$

The difference in solute concentration drives the Osmotic potential while hydrostatic pressure conveys the pressure potential and gravitational potential is governed by the elevation relative to a reference datum.

Generally, it is accepted that the kinetic energy of the water movement in soils is unaccounted for due to the extremely slow velocity; moreover, pressure and gravitational potentials are considered negligible due to the arbitrary reference.

The contribution of the matric potential in soil suction has the most remarkable function. It arises from the effects of capillary action, as discussed in the previous discussions, combined with adsorptive effects contained in a soil matrix.

The so-called potential, which is referred to as “suction” is a constitution of the matric and osmotic components.

$$T = M + O \quad (9)$$

2.2 Soil-Water Characteristic Curve

The soil-water characteristic curve is the relationship between water content and suction for the soil. Proper and accurate characterization is required since it has been a basis for the prediction of other unsaturated soil properties such as hydraulic conductivity and shear-strength parameters. It has become essential in the application of unsaturated soil mechanics in geotechnical engineering. (Fredlund, 1994; Fredlund, Sheng et. al, 2011)

2.2.1 Typical Components and Shape

Fredlund, et. al (2011) emphasized on the SWCC as expansively employed for the estimation of the property functions of unsaturated soils.

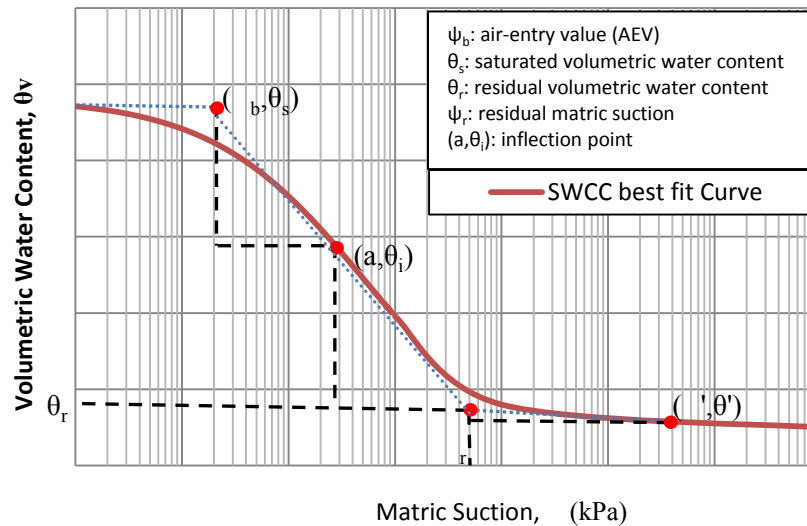


Figure 2.7: Definition of variables from SWCC (Zhai et.al, 2012)

The nature of SWCC is known to have two distinct changes which are the air-entry value and residual conditions. It is the zone between these two where the slope is sufficient for calculation. Figure 2.7 illustrates the graphical solution for the estimate of curve parameters.

It is also highlighted that there is a hysteretic nature of SWCC. It states that it is not possible to determine a single stress state designation which is unique for a soil; based solely on its gravimetric water content. Stated as there are uncertainties to determine if you are in the drying, wetting or scanning curve.

There are several factors influencing the SWCC, such as initial water content, dry density and consolidation pressure. It is also important to bear in mind that soil mineral composition, pore structure, stress history and temperature mainly affect the SWCC behavior.

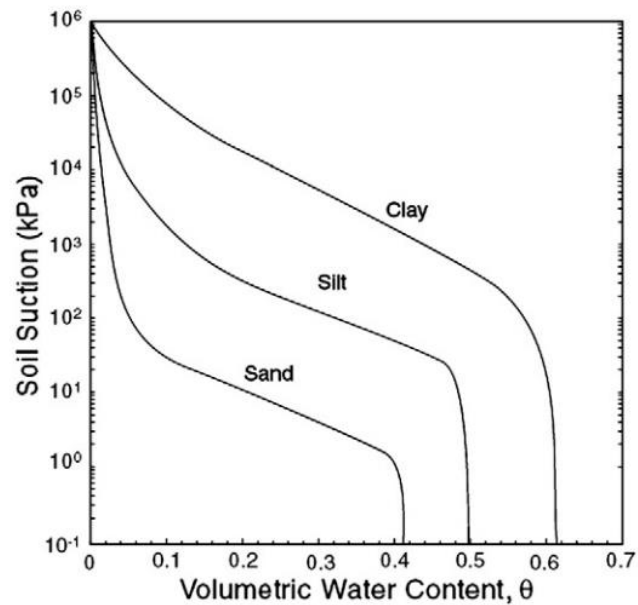


Figure 2.8: Typical curves of SWCC (Lu and Likos, 2004)

The typical shape and range of suctions are given in Figure 2.8. Sand, having low water storage capacity has the lowest volumetric water content at saturation while clay, being porous and possessing a large specific surface and adsorption capacity has the largest volumetric water content.

Two models were particularly selected from the *Equations of the soil-water characteristic curve* published by Fredlund and Xing in 1994 to fit the experimental data the three equations chosen are: Van Genuchten (1980) and Fredlund & Xing with correction (1994) models. These equations have already established good correlation for a wide range of suction and various soil types.

2.2.2 Fredlund and Xing with correction factor (1994)

Equation (10) was derived from a frequency distribution which can measure the range from 0 to 10^6 kPa, developed by Fredlund and Xing in 1994.

$$\theta = \theta_s \left[1 - \frac{\ln\left(1 + \frac{\psi}{\psi_r}\right)}{\ln\left(1 + \frac{10^6}{\psi_r}\right)} \right] \left[\frac{1}{\left\{ \ln\left[e + \left(\frac{\psi}{a}\right)^n \right] \right\}^m} \right] \quad (10)$$

where:

a = curve fitting parameter related to the air-entry value.

n = curve fitting parameter related to the slope of the curve; a higher value leads to a steeper slope as clarified in Figure 2.9. It may be related to the rate of desaturation of the soil as the soil suction exceeds air-entry value.

m = curve fitting parameter related to the residual water content; inversely related to the residual water content as seen in Figure 2.10.

θ_s = saturated volumetric water content.

θ_r = residual volumetric water content.

ψ = suction applied

ψ_r = residual suction

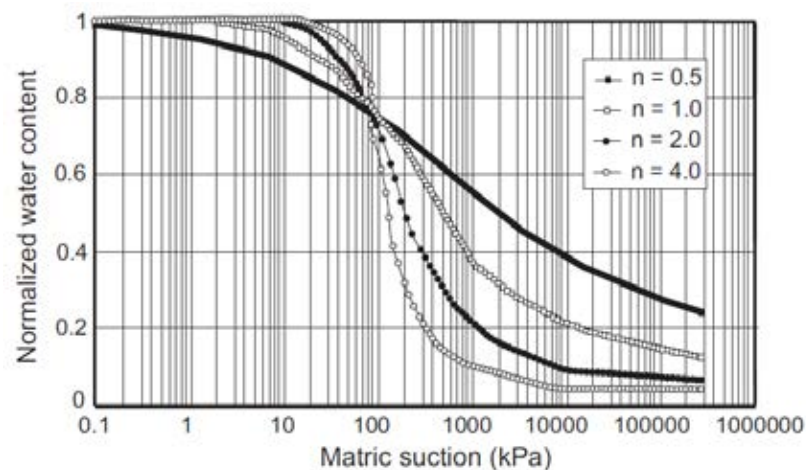


Figure 2.9: Sample plot for the effect of n parameter (Fredlund and Xing, 1994)

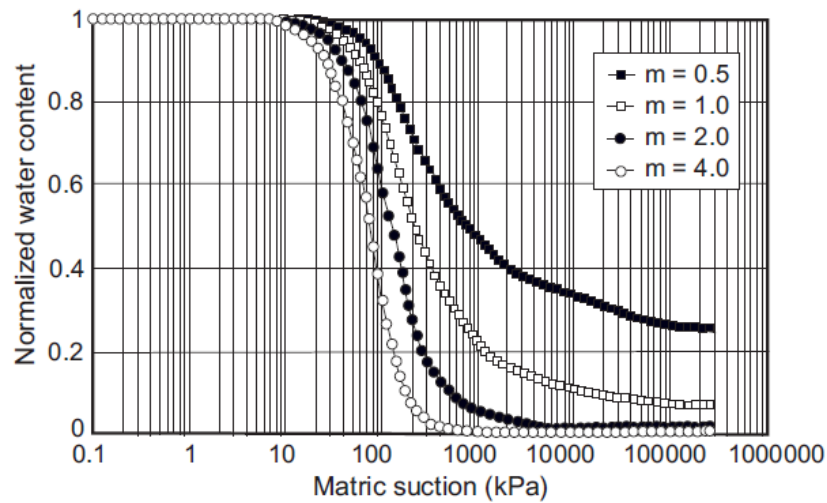


Figure 2.10: Sample plot for the effect of m parameter (Fredlund and Xing, 1994)

2.2.3 Van Genuchten (1980)

A very flexible equation which is frequently used for the relationship between suction and normalized water content is the Van Genuchten (1980) which will be referred as equation (11):

$$\theta = \theta_r + (\theta_s - \theta_r) \left[\frac{1}{1 + \left(\frac{\psi}{a} \right)^n} \right]^m \quad (11)$$

where:

a , n and m = different curve fitting parameters

$m = (1 - 1/n)$; m and n were related by van Genuchten in an attempt to obtain a closed-form equation for hydraulic conductivity. Fredlund and Xing in 1994 however, emphasizes that this relationship reduces the flexibility of the equation suggesting that it would be more accurate to leave the two parameters unrelated (i.e, no fixed relationship between m and n).

θ_s = saturated volumetric water content

θ_r = residual volumetric water content

2.3 Instrumentation and Measurement

Quantification of soil suction may be classified into direct and indirect methods; the former, as the name implies, is capable of promptly measuring negative pore water pressure while the latter essentially derives suction from interrelated parameters such as RH, hydraulic conductivity and water content.

The direct method (i.e tensiometers, axis-translation, etc) however, is only capable of measuring matric suction and necessitates a good contact between the sensor and the sample while the indirect method can measure both matric and osmotic suction.

Pan, Qing and Pei-Yong (2010) reviewed various techniques which have been widely used in research laboratories as well as in engineering practice.

Table 2.1: Summary of suction measurement methods
(Pan, Quin and Pei-Yong, 2010)

		Technique (Method)	Suction Range (kPa)	Equilibrium Time	
Direct Method	Matric Suction	Axis-translation Technique	0 to 1500	hours	
		Tensiometer		hours	
		Suction Probe		minutes	
Indirect Method	Matric Suction	Time Domain reflectometry	0 to 1500	hours	
		Electrical Conductivity Sensor	50 to 1500	6 to 50 hours	
		Thermal Conductivity Sensor	0 to 1500	hours to days	
		In-Contact Filter Paper	all	7 to 14 days	
	Osmotic Suction	Squeezing Technique	0 to 1500	days	
	Total Suction		Psychrometer Technique	100 to 10,000	1 hour
			Relative humidity sensor	100 to 8,000	hours-days
			Chilled-Mirror Hygrometer	150 to 30,000	10 minutes
			Non-Contact Filter Paper	all	7 to 14 days

2.3.1 Pressure Plate Extractor (0 to 1500 kPa)

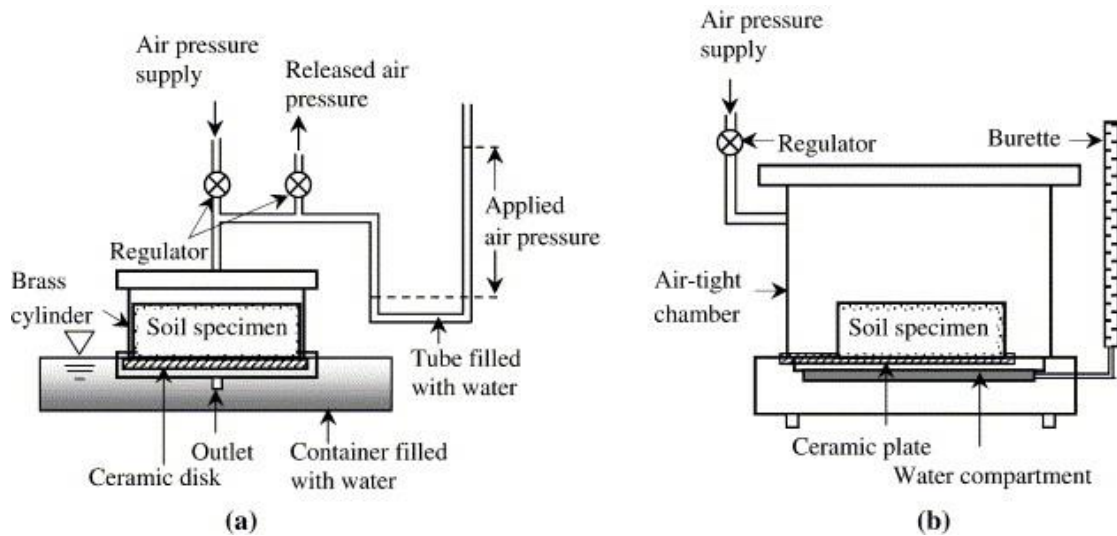


Figure 2.11: Pressure plate extractor system. (Indrawan, 2006)

The Pressure plate apparatus shown in Figure 2.11(a) operates on suctions from 0 to 100 kPa; it may take a long time to reach equilibrium in an undisturbed, full-size core.

ASTM D6836-0 describes these as Method B (pressure chamber with volumetric measurement) and Method C (pressure chamber with gravimetric measurement) are suitable for suctions in the range of 0 to 1500 kPa.

It functions by the axis-translation technique; thru increasing the air pressure in the chamber, a corresponding escalation of water pressure in the soil approximately equal to the difference in the air pressure in the chamber and atmospheric pressure takes place. If suction is held constant inside the chamber, water will drain out of the specimen and recurring measurements of volume or weight may be taken.

2.3.2 Tensiometers (0 to 100 kPa)

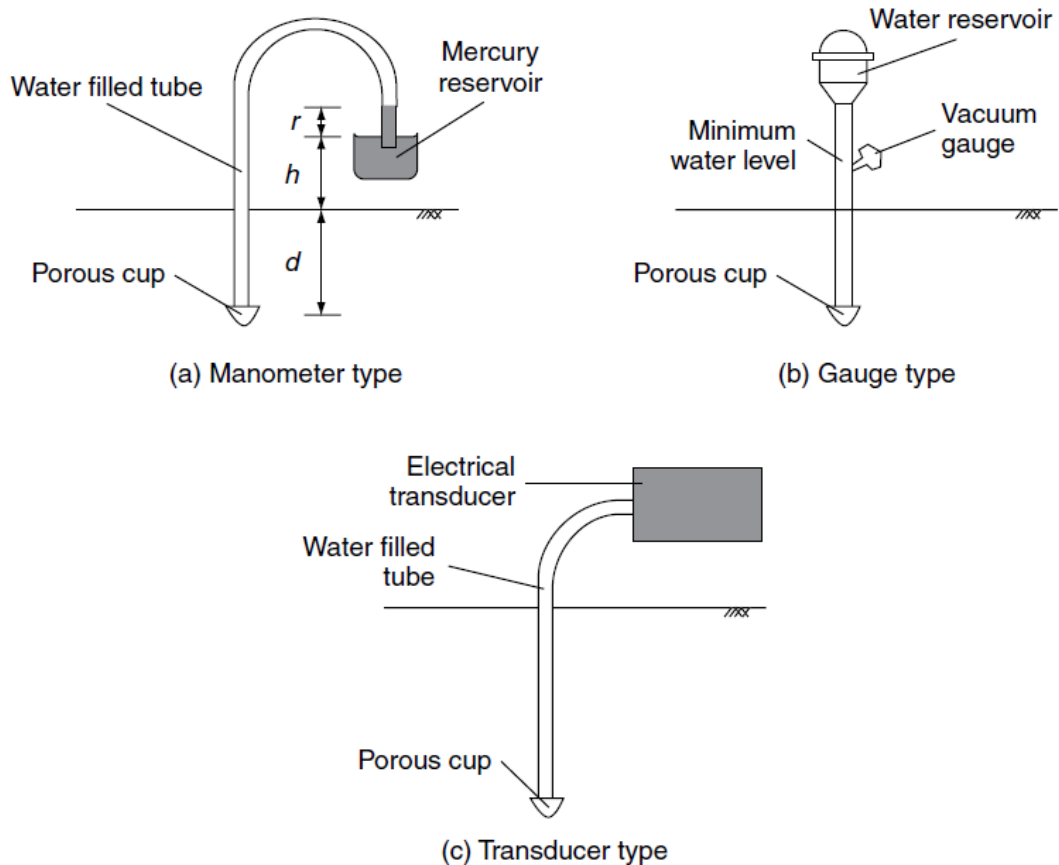


Figure 2.12: Common types of tensiometer configurations (a) manometer type (b) gauge type (c) transducer type (Ng et.al, 2007)

The apparatus operates on the principle of attaining equilibrium between a soil sample and water by utilizing a high air entry material such as a ceramic stone cup filled with de-aired water. The fluid in the reservoir is allowed to be extricated through the ceramic cup up to the point that the suction in the fluid inside the probe is in equilibrium with the suction present in the soil. No further exchange or flow of fluid will be manifested at this point. Figure 2.12, (i.e. manometer, Bourdon gauge, and transducer) presents the measuring devices which are responsible for evaluating the pressure values during the test. The simplicity and convenience of the device are valuable but similar to any device, this also has limitations. Biased results of pore water pressure may occur due to the presence of air in the sensor.

2.3.3 Hanging Column (0 to 100 kPa)

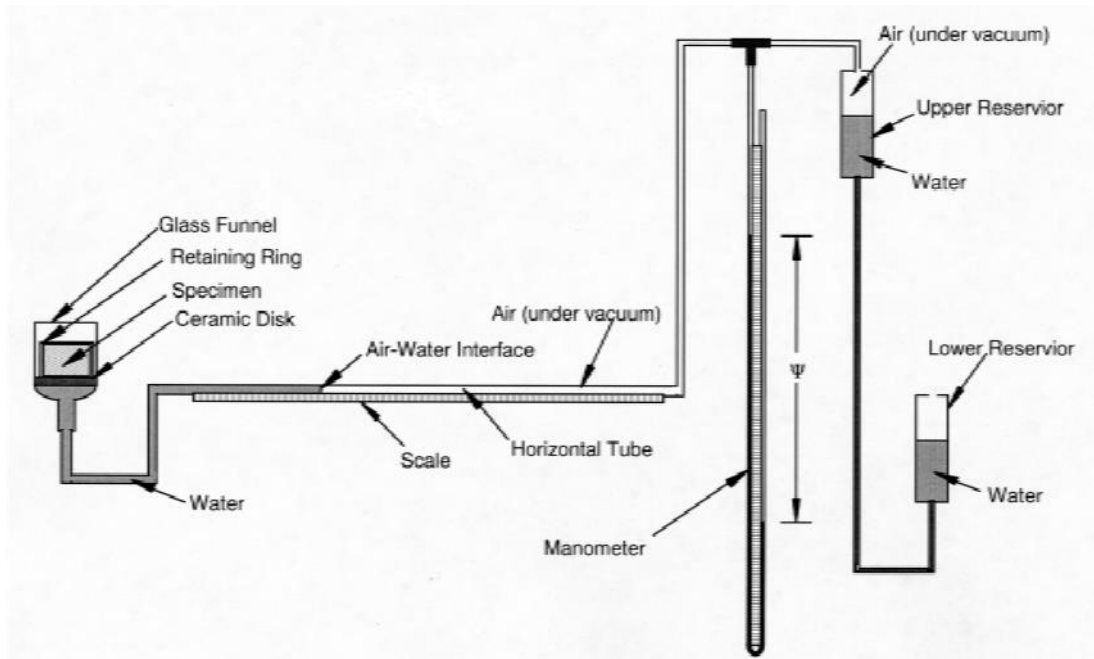


Figure 2.13: Schematic diagram of a hanging column apparatus (ASTM D 6836-02)

The apparatus is basically composed of a specimen chamber, an outflow measuring tube and a suction supply. Buchner funnels generally contain porous plate that is capable of securing the specimen chamber. The water pushed out of the specimen is connected to the outflow end of the funnel, where the corresponding other end is connected to a suction supply. The suction is a product of two fluid reservoirs whose elevations are adjusted to generate a vacuum which is measured by a pressure measuring device (i.e. manometer).

The porous plate and the soil sample must have good contact. Equilibrium time for the porous plate and the soil specimen requires at least 48 hours and every pressure increment compels at least 24 hours before the next suction is applied.

2.3.4 Filter Paper (Entire Range of Suction)

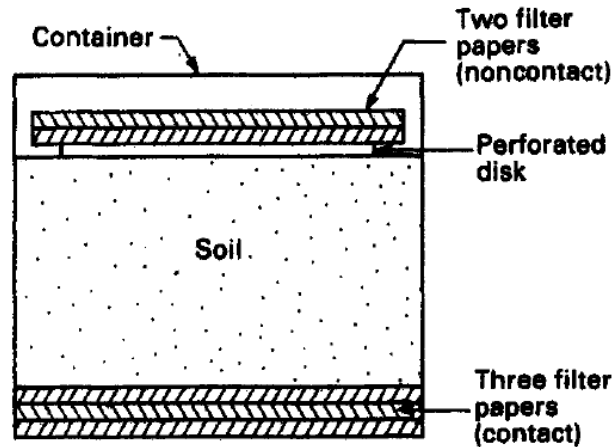


Figure 2.14: Contact and noncontact filter paper methods for measuring matric and total suction, respectively. (Fredlund, 1993)

Pioneered by the field of soil science, the method determines the amount of water transferred from the unsaturated specimen to the dry filter paper until it reaches equilibrium. The non-contact method is employed if the total suction is to be known while the contact filter paper is adapted to survey the matric suction. Subsequent to the unique calibration curve of the filter paper, the water content is then associated in correlation to the selected curve.

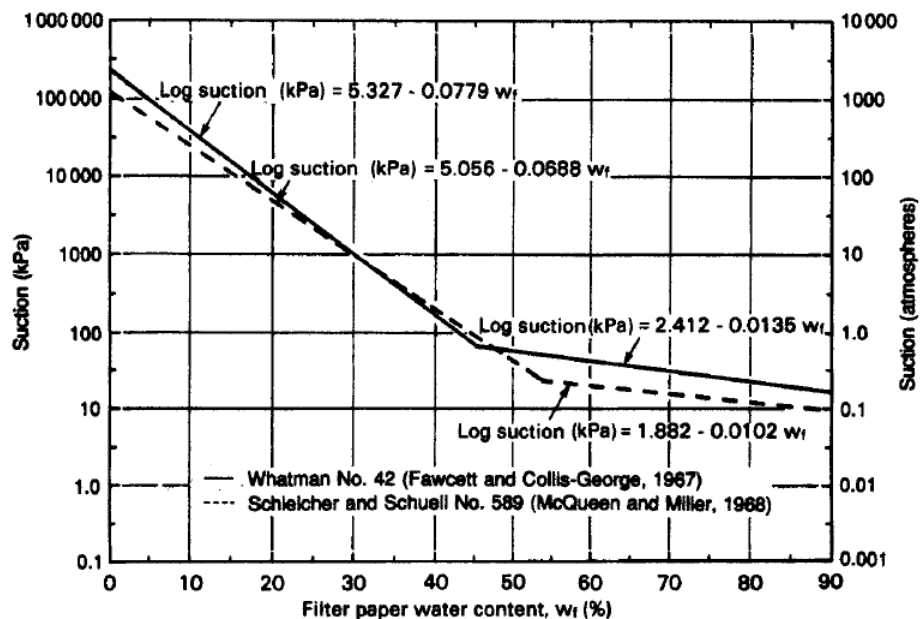


Figure 2.15: Calibration curves for two types of filter paper. (Fredlund, 1993)

2.3.5 Unified measurement system with suction control

A unified measurement system as shown in Figure 2.16 was developed in 2012 by Rouf et. al., it was through improvising five apparatuses integrated into one device that can obtain measurements for both SWCC and gas transport parameters. A moisture sensor is installed to monitor the volumetric water content of the soil while the suction was produced through supplying different suction heads. By increasing the head, the drying curve can be determined and the wetting curve by reversing the process.

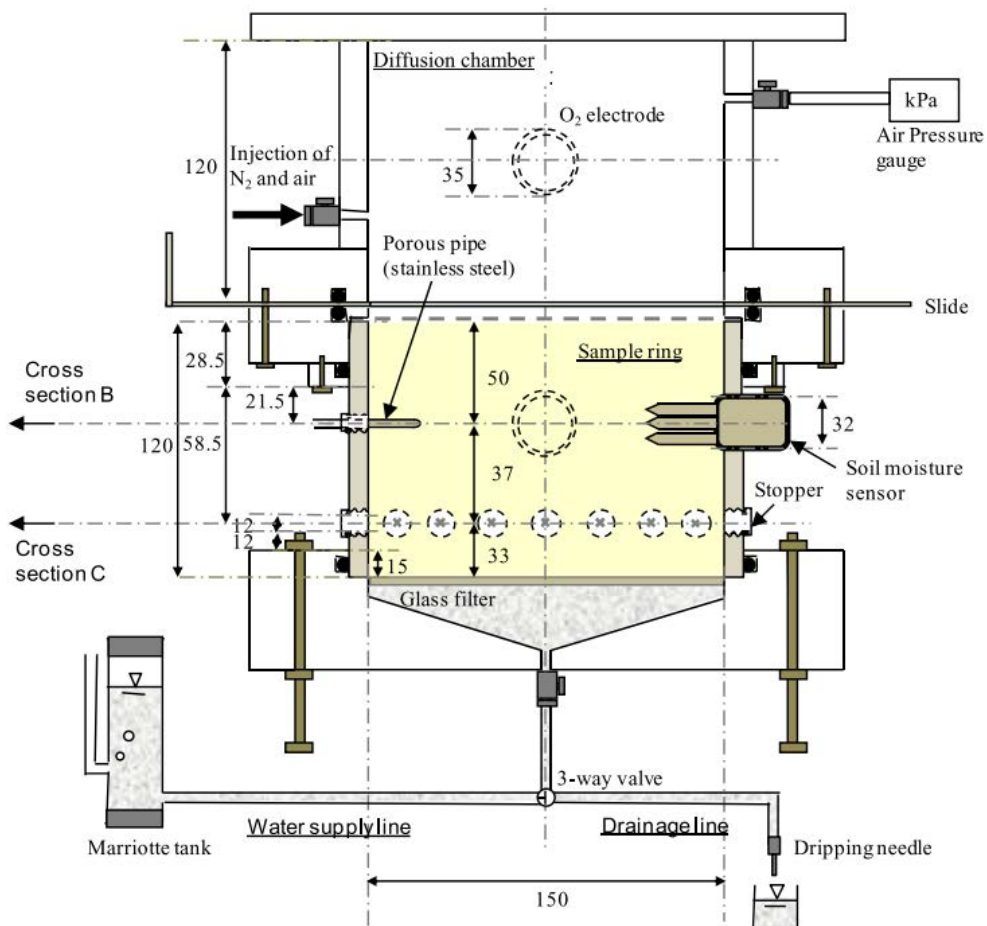


Figure 2.16: Unified measurement system with suction control (Rouf, et. al., 2012)

2.4 Unsaturated Shear Strength Criteria

The saturated shear strength are conventionally based on the Mohr-Coulomb failure denoted by equation (12) which is actually extended by many researchers to accommodate the contribution of pore pressures (i.e matric suction) as illustrated in Figure 2.17. Predictions for the unsaturated shear strength together with their closed for solutions were discussed by Fredlund et al. (1995).

$$\tau = c' + (\sigma - u_w) \tan \phi' \quad (12)$$

Shear strength for unsaturated soils under wetting and drying conditions were completely discussed by Guan et al. (2010) where several types of equations for shear strength were categorized under fitting or prediction. The equation (13) by Fredlund et al. (1978) given by: $\tau = c' + (\sigma - u_w) \tan \phi' + (u_a - u_w) \tan \phi^b$ (13) was adapted for this study.

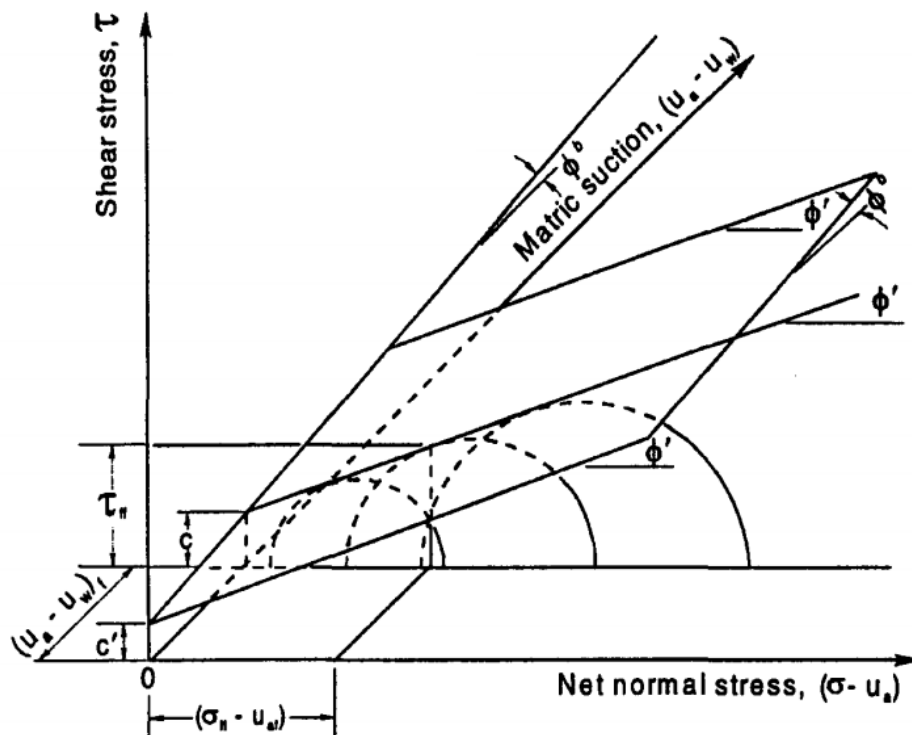


Figure 2.17: Extended shear strength for unsaturated soils (Fredlund, 1993)

The parameter ϕ^b which is the angle of friction with respect to suction can be related to the angle of internal friction ϕ' by a fitting parameter λ' by:

$$\lambda' = \frac{\tan \phi^b}{\tan \phi'} \quad (14)$$

Khalili and Khabbaz (1998) suggested this parameter to be equal to equation (15) to accommodate the normalize non-linear contribution of suction to the strength:

$$\lambda' = \left\{ \frac{(u_a - u_w)}{(u_a - u_w)_b} \right\}^{-0.55} \quad (15)$$

2.5 Existing works

Nuntasarn et. al. (2011) investigated the relationship between the soil suction and unconsolidated undrained (UU) shear strengths of unsaturated Khon Kaen loess. Basic properties of Khon Kaen Loess, a collapsible soil, were evaluated in addition to the SWCC as presented in Figure 2.18 obtained by the hanging column, pressure plate and isopiestic humidity method performed on a compacted specimen.

Ten samples were remoulded and compacted into 50mm by 100mm specimens with an initial γ_d of 1.7t/m³ and gravimetric moisture of 14%. The undrained shear strength was determined by unconsolidated undrained test (UU test) at a confining pressure of 100 or 200 kPa. Two of the samples were tested right after preparation by compaction while the other eight samples were naturally dried for 2, 12, 24 or 72 hours preceding undrained shear. However, no measurements were provided for both pore air and pore water so the UU test was related to the total stress. The saturated UU test total friction angle was measured at 0° degrees however there was an exponential relationship established between the soil suction and shear strength.

Punrattanasin et. al. (2002) established the Engineering properties of Khon Kaen loess under unsaturated condition and also produced an SWCC in Figure 2.20. They tested both disturbed and undisturbed samples in Thailand and Japan; measured SWCC by the pressure plate method together with the vapour equilibrium technique. The air-entry value for the Khon Kaen loess was found at about 25 kPa while the residual water content and residual suction of the were 5% and 500 kPa, respectively.

The test showed that the effective cohesion c' is zero and the angle ϕ_b is equal to 32° however, the contribution of suction in residual state suction appeared to be constant.

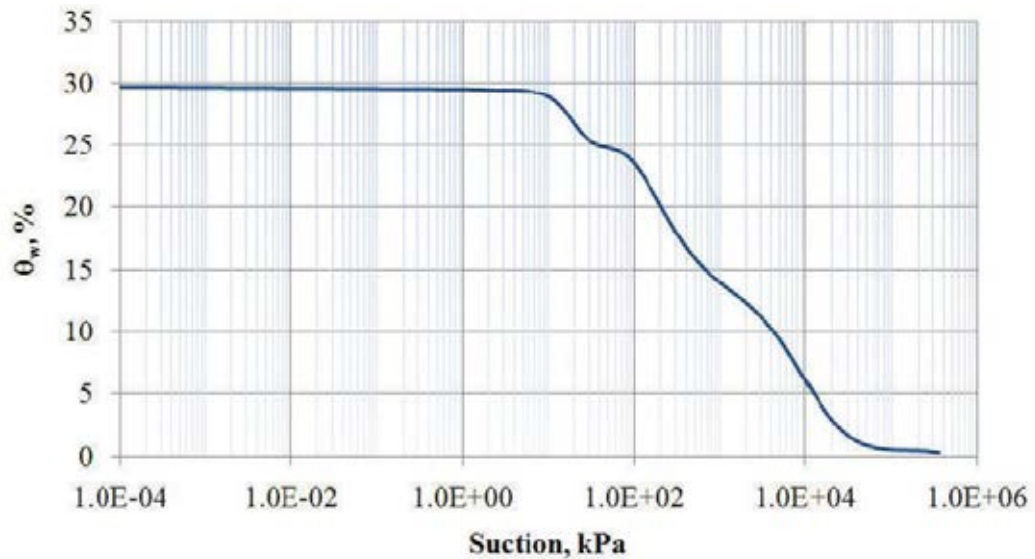


Figure 2.18: SWCC of compacted khon kaen loess by hanging column, pressure plate and isopiestic humidity method (Nuntasarn, 2011)

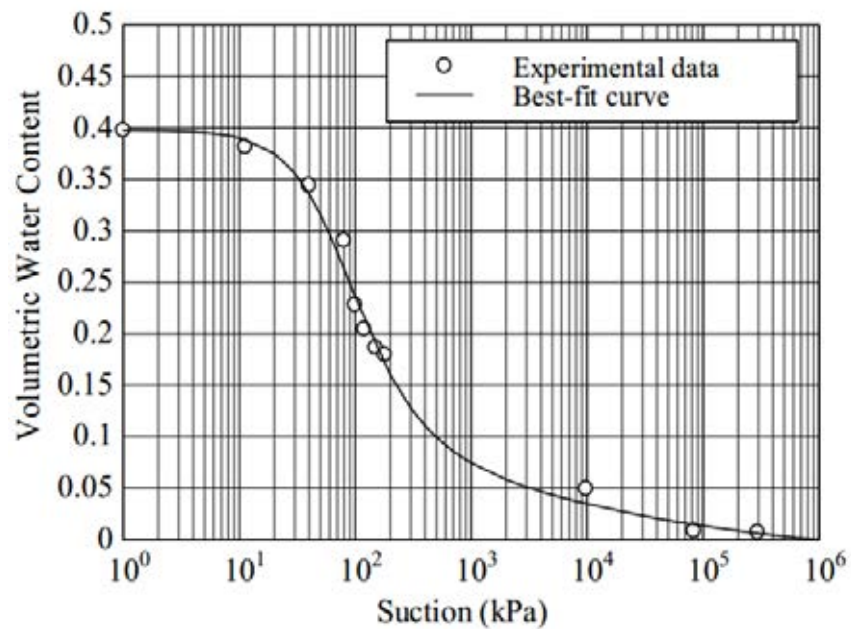


Figure 2.19: SWCC of Khon Kaen loess by Pressure plate method and Vapour equilibrium technique (Punrattanasin et. al, 2002)

2.6 Multiple Regression

In cases when more than one variable is necessary to statistically model a given situation, the general multiple regression model is given by: $Y = \beta_0 + \beta_1x_1 + \beta_2x_2 + \varepsilon$ (16). It is expected that the Y variable will be predicted after analysing the given regressors. The beta coefficients are intended to give the weight of the independent variables to be able to best predict the dependent variable. Statistics of Analysis of Variance (ANOVA) provide the hypothesis testing to see if the regression may be accepted or not.

2.6.1 Least Square Estimation of the Parameters

In order to estimate the function best fitting model, minimizing L in the equation: $L = \sum_{i=1}^n \varepsilon_i^2 = \sum_{i=1}^n (y_i - \beta_0 - \sum_{j=1}^k \beta_j x_{ij})^2$ (17) with respect to $\beta_0, \beta_1, \dots, \beta_k$. If this is differentiated with respect to the respective parameters, the least squares normal equations (18) to (20) will solve the system of multiple equations:

$$n \hat{\beta}_0 + \hat{\beta}_1 \sum_{i=1}^n x_{i1} + \dots + \hat{\beta}_k \sum_{i=1}^n x_{ik} = \sum_{i=1}^n y_i \quad (18)$$

$$\hat{\beta}_0 \sum_{i=1}^n x_{i1} + \hat{\beta}_1 \sum_{i=1}^n x_{i1}^2 + \dots + \hat{\beta}_k \sum_{i=1}^n x_{i1} x_{ik} = \sum_{i=1}^n x_{i1} y_i \quad (19)$$

$$\hat{\beta}_0 \sum_{i=1}^n x_{ik} + \hat{\beta}_1 \sum_{i=1}^n x_{i1} x_{ik} + \dots + \hat{\beta}_k \sum_{i=1}^n x_{ik}^2 = \sum_{i=1}^n x_{ik} y_i \quad (20)$$

Table 2.2: Multiple Regression Data Lay-out (Montgomery, 2003)

y	x ₁	x ₂	...	x _k
y ₁	x ₁₁	x ₁₂	...	x _{1k}
y ₂	x ₂₁	x ₂₂	...	x _{2k}
...
y _n	x _{n1}	x _{n2}	...	x _{nk}

2.6.2 Hypothesis Testing in Multiple Linear regression

In order to determine whether there is actuality in the linear relationship between the regressors and the dependent variable, the applicable hypothesis is given by: $H_o : \beta_1 = \beta_2 = \dots \beta_k = 0$ and $H_1 : \beta_j \neq 0$ for at least one j . If the F-Stat value falls inside the region of acceptance, it means that there is no significant contribution of the regressors to the model. On the other hand, if the F-stat value is in the excluded area, there is at least one variable that principally contributes to the model. Where the F-stat value, F_o , is given by dividing the Mean Square of the Residual, by the Mean Square of the Error. The table for acceptance is given in the Appendix.

2.6.3 R-squared

The so-called R^2 or *coefficient of multiple determination* is a measure of how much of the variables are accounted for in the model. The higher percentage corresponds to a better value; a value closer to 1 or 100% accountability is desired. The relationship was derived from:

$$R^2 = 1 - \frac{SS_E}{SS_T} \quad (21)$$

where:
$$SS_E = \sum_{i=1}^n (y_i - \hat{y}_i)^2 \quad (22)$$

$$SS_T = \sum_{i=1}^n (\hat{y}_i - \bar{y})^2 \quad (23)$$

CHAPTER III METHODOLOGY

3.1 Materials



Figure 3.1: Soil Sampling. (a) The response of shredding of the soil due to evaporation in the topsoil layer and (b) shows the test pit at 2.50 meters to 3.00 meters at Khon Kaen University (c) the fragility of the soil sample (d) manual block sampling done.

The soil specimen was obtained from Khon Kaen University in Muang Khon Kaen, located in the North-eastern part of Thailand. Due to its collapsible nature, block sampling was required for 2.50 to 3.00 meters from the ground surface, 30 samples were dug from the ground and cut into 6" x 12" cylinder samples. Laboratory

tests were performed in the Geotechnical Laboratory, ground floor of the Civil Engineering Building at Chulalongkorn University, Bangkok, Thailand.

3.1.1 Preparation of Sample for testing

In preparation for the triaxial test, the samples were trimmed into *undisturbed* cylindrical specimens with a target size of 70 mm. diameter and a length of 140 mm with an error band of ± 3 mm. The gravimetric water content was measured for at least three parts: top, bottom and sides. Specimens are visually examined for cracks and the presence of other debris (e.g. roots), the presence of cracks due to disturbance or any other reasons deems the specimen inappropriate for testing and a new specimen was trimmed.

A ceramic stone is attached to the base pedestal, a Whatman #1 qualitative filter paper is placed on top of the disc, and then the specimen is positioned. Suction is applied to a membrane suction device to carefully attach the membrane then three O-rings are attached at the bottom. A porous disc and a top load cap are placed on top then two O-rings are then used to finally seal the specimen. This is immediately placed on the frame, and then subjected to four stages of testing which will be discussed in detail in the next two sections.

3.2 Instrumentation

To be able to accurately measure the SWCC by providing matric suction, a 50kN Wykeham Farrance Unsaturated Triaxial System was used. It is a modified triaxial system designed in such a way to accommodate the changes required to produce both the pore air and pore water pressures. The system is composed of a double triaxial cell, two automatic volume change devices, two hydraulic pressure controllers and an air pressure controller which are all connected to an RTC and ATD Data logger that is automatically controlled by a computer software system. Figure 3.2 shows the basic set-up of the system.

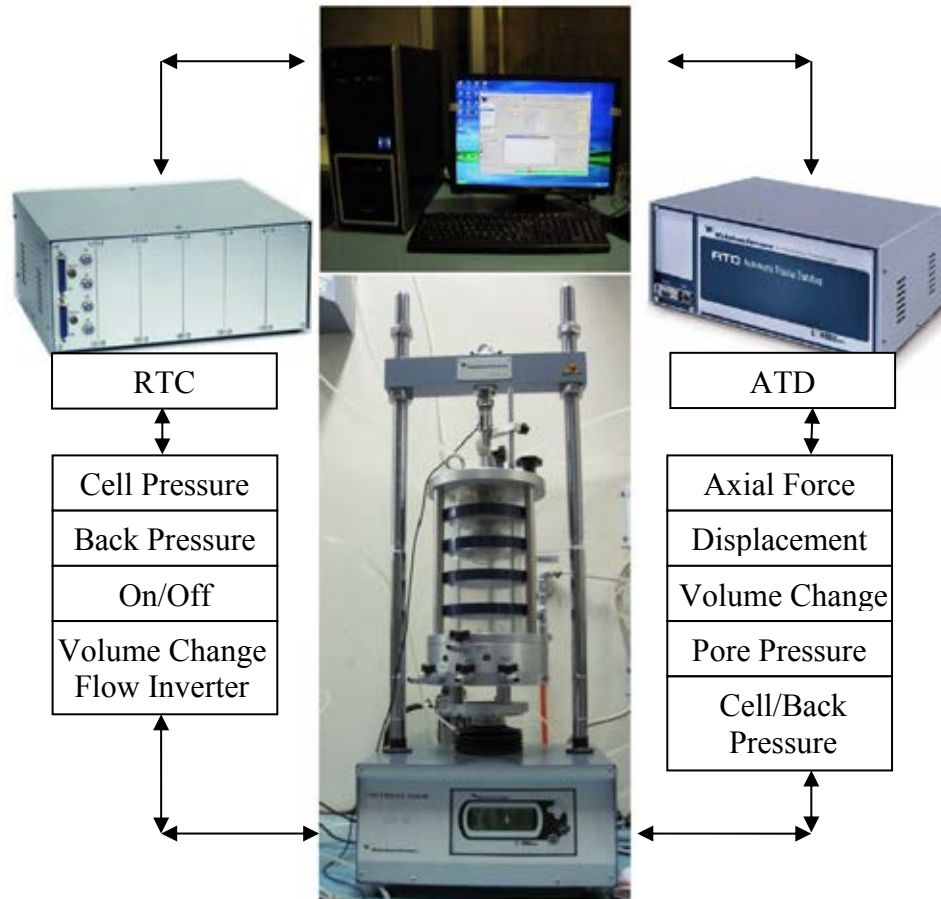


Figure 3.2: The unsaturated triaxial system set-up

The Real-Time Control (RTC) box functions as the “brain” of the Automatic Triaxial System which comprises a chassis with a base RTC module which allows control of the triaxial system. It controls two hydraulic pressure lines, open and close the two solenoid valves of the pressure lines, control the speed of the triaxial load frame and invert the flow direction of the automatic volume change device.

The Automatic Triaxial Datalog (ATD) is required for the transmission of the transducer values, via the high-speed communications network, to the RTC box and the computer running the testing and also the management software.

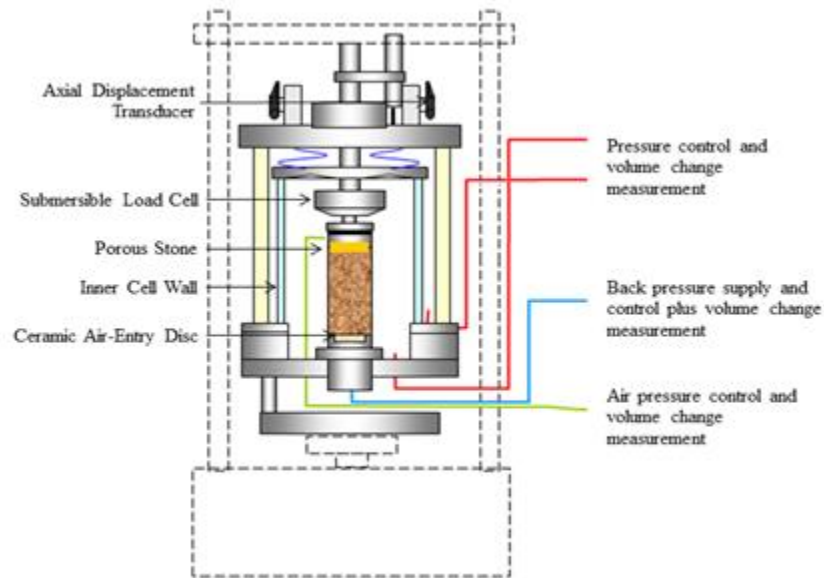


Figure 3.3: The triaxial cell diagram with air and water connections (Wykeham Farrance, 2010)

The double cell wall is comprised of a Perspex outer cell chamber while the inner cell is made of glass to ensure that the volume change is a product of the soil sample and not from any other sources. It runs on a working capacity of 2000 kPa.

The base pedestal of the cell chamber has 6 ports which has specific purposes. If it is attached to the system, four ports are facing the front in which the first one is for the inner cell, the second is for back pressure, the third one is for saturation port or pore pressure measurement above the ceramic stone and the last one is for the outer cell pressure chamber. At the rear part, the air valve and pore pressure measurement port are located.

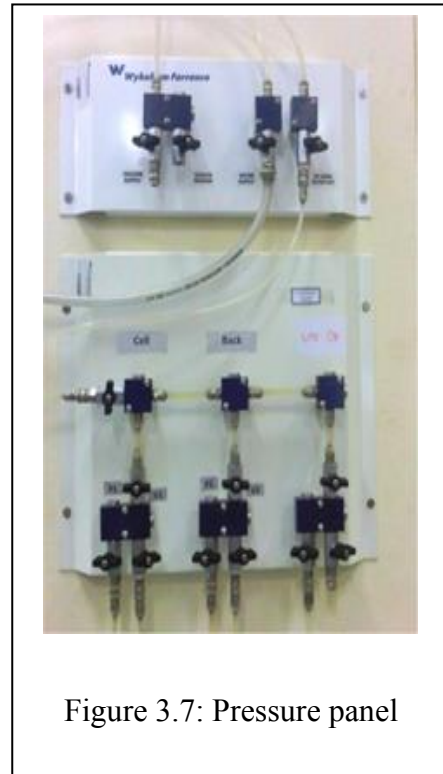
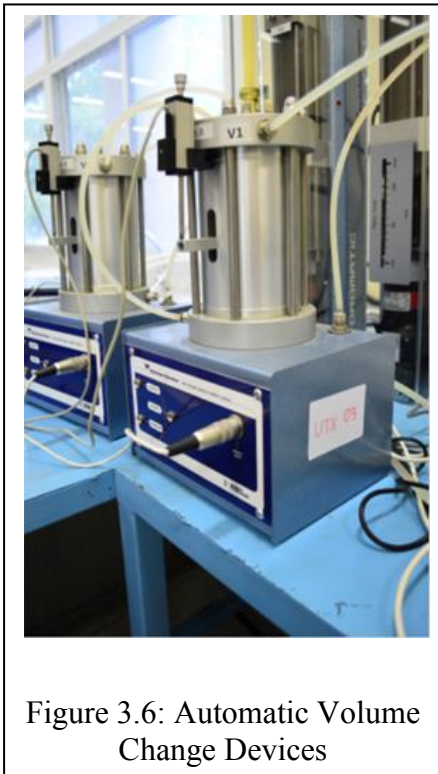


Figure 3.5 shows the Air Pressure Controller which controls the air pressure for the specimen consists of a base system that is capable of controlling pneumatic pressures up to 1000kPa on the pressure line. The unit runs on an input air-supply and contains an electro-pneumatic control valve that regulates the supply in direct proportion to a signal received from the RTC box. Since the attached available air compressor produces a maximum 700 kPa, the maximum air pressure that we will utilize will be 500 kPa to ensure safety of the system.

In Figure 3.4, Two Hydraulic Pressure Controllers are illustrated which are necessary to generate the cell and back pressures. Each unit contains approximately 250cc of water and capable of generating up to 3500kPa of pressure. The pressure is generated by means of a hydraulic piston which is driven by a stepper motor.

The Automatic Volume Change device as seen in Figure 3.6 comprises a piston sealed within a water-filled chamber, connected to a 25mm linear displacement transducer.

A flow of water through the unit causes movement of the piston which is measured by the transducer. The output of the transducer is directly proportional to the volume of water flowing through the unit. The unit contains integral solenoid valves to allow automatic control of the flow direction functions. It is powered and controlled by the RTC box which responds to feedback from the unit's linear displacement transducer to enable continuous volume change to be measured.

The pressure panel is not only used to divert and control the flow of water from the source of de-aired water tank to the system but also regulate the flow from the pressure controllers to the double cell walled chamber. The image of the panel is seen in Figure 3.7.

3.3 Triaxial Stages

3.3.1 Saturation

To initialize the testing, from its natural water content, which ranges from 8 to 9 %, saturation were performed unto the *undisturbed* samples by applying increments of cell and back pressure. With an initial void ratio which is comprised of combined air and water; air which is a compressible fluid and water being incompressible.

Cell pressure was applied in increments of 50 kPa in accordance to BS 1377 then a back pressure with a difference of 10 kPa was applied. Saturation was calculated by the amount of water that flowed inside the specimen. Moreover, the B-value is given by equation (24) where the specimen was then said to be saturated if B-value is reported as 0.95 or greater.

$$B = \frac{\Delta u_w}{\Delta \sigma_3} \quad (24)$$

Running on software also gave the advantage of being able to measure the amount of water that went inside the sample, making accurate back calculations possible.

3.3.2 Isotropic Consolidation

In preparation of the soil sample for the soil-water characterization, it is necessary to carry out the designed stresses. By altering the difference between the cell pressure and the back pressure, the net stress would then be acquired.

The excess pore pressure had to be dissipated by minimizing the pore water pressure value that is greater than the back pressure. By opening the back pressure

valve and allowing the pore water pressure to decrease until such time and equilibrium will be attained between the two.

This step is very important for the test since the difference between the cell pressure and the back pressure will dictate the maximum range of matric suction that could be possibly applied since the air pressure should be equal or less than cell pressure.

3.3.3 Soil-Water Curve Stage

As discussed in the previous chapter, the difference between the pore air and water pressure, $u_a - u_w$, known as the matric suction together with the change in water content were measured.

Air pressure was increased by increments ranging from 5 to 40 kPa and then this was held until the pressures are stable. It was repeated until no change in water volume is recorded, and equilibrium was attained. After the completion of desired suctions, the assumption is made that the drying curve has already been completed.

3.4 SWCC Construction

After obtaining the data points, the void ratio and degree of saturation were used to convert the gravimetric water content to the volumetric equivalent. The data was plotted and the parameters such as the air-entry value, slope of the curve and residual water content were graphed. These were plotted utilizing the two models described in the previous chapter to be able to obtain the SWCC curve for Khon Kaen Loess. The sum of squared residuals, also referred to as SSR, was also used for best fitting the data.

3.5 Shear Strength Analysis

The given cohesion and angle of internal friction values of soils were used in the analysis; while the soil suction was estimated from the tested SWCC.

The void ratio, degree of saturation, gravimetric water content and specific gravity were used for conversion of soil data to volumetric water content. The data combined were used for the fitting and prediction of unsaturated shear strength. Linear multiple regression was applied to predict the standardized plane surface.

CHAPTER IV

RESULTS AND DISCUSSIONS

4.1 Review of Fitting equations

For clarity purposes, the main fitting equations for the suction data discussed in section 2.2.2 and 2.2.3 are presented again with their corresponding denotations. For both equations, a , m and n are fitting parameters while θ_s is the saturated volumetric water content and θ_r is the residual volumetric water content. These were be used for modelling both sands and loess.

The Fredlund and Xing (1994) equation will be referred as Model (1) where ψ is the suction applied and ψ_r is the residual suction.

$$\theta = \theta_r + (\theta_s - \theta_r) \left[\frac{1}{1 + \left(\frac{\psi}{a} \right)^n} \right]^m$$

The Van Genuchten (1980) equation will be referred as Model (2).

$$\theta = \theta_r + (\theta_s - \theta_r) \left[\frac{1}{1 + \left(\frac{\psi}{a} \right)^n} \right]^m$$

4.2 Calibration of Unsaturated Triaxial Test with standard sand

This section discusses the use of standard sands for the calibration of the system and how the values might differ using other conventional apparatuses. Properties and experimental results of unsaturated triaxial testing are presented and modeled to conform to the paradigms of unsaturated soil mechanics.

4.2.1 Toyoura and Ottawa sand

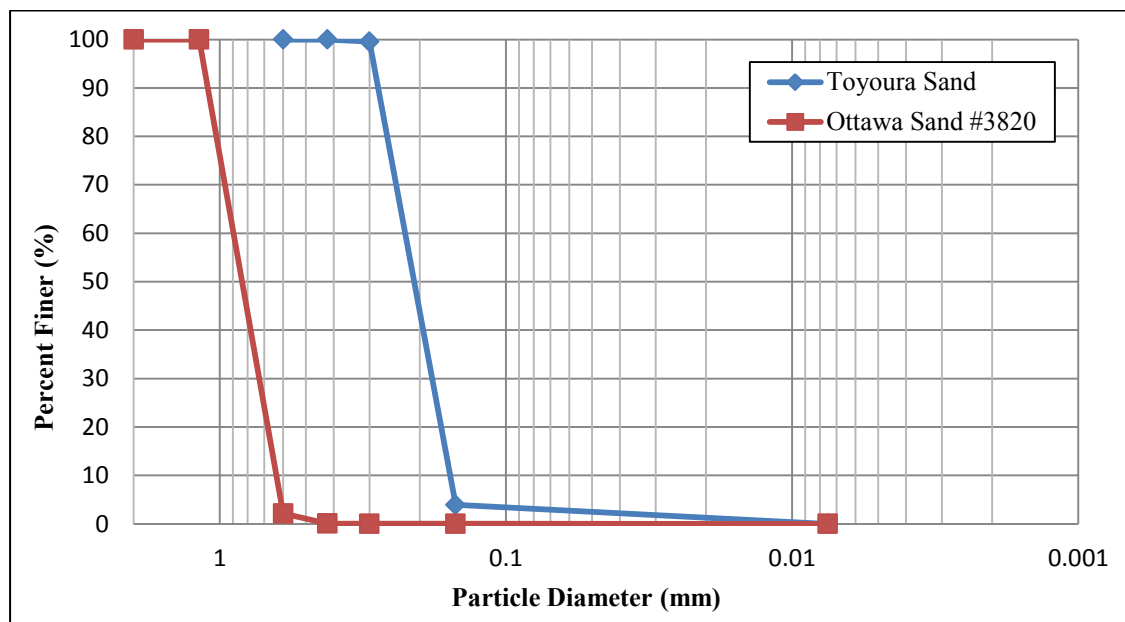


Table 4.1: Properties of tested sands

Property	Toyoura Sand	Ottawa Sand
Specific gravity, G_s	2.64	2.64
Mean grain size (D_{50}), mm	0.210	0.835
Coefficient of uniformity, C_u	1.433	1.414
Coefficient of curvature, C_c	1.011	0.933

4.2.2 Designation of Tested Sands

The data sets have had been divided into 5 test sets with labels as assigned in Table 4.2.

Table 4.2: Designation of Tested Sands

Sample	Designation	Applied Cell Pressure, σ_3	Pore Water Pressure, u_w
Toyoura sand	T1	500	100
Toyoura sand	T2	500	200
Toyoura sand	T3	500	300
Ottawa sand	O1	500	100
Ottawa sand	O2	500	200

4.2.3 Results of SWCC

After applying air pressure with initial increments of 5kPa, Toyoura sand with a D_{50} of 0.210mm was able to withstand an applied suction in the first step, with a sustained volumetric water content of 32%, the smaller particles provide more adhesion area for the water molecules but after application of further suctions, the residual state comes into place. No remarkable loss of water content was observed even after the increasing the matric suction up to 100 kPa. Figure 4.2 exhibits the test points of the study. This is an indication that under confined conditions, a pendular state of saturation occurs in the residual conditions of Toyoura sand but not for Ottawa Sand.

Ottawa Sand, in this case obtained a dry state, with the first application of a matric suction of 5kPa, the volumetric water content had a null value. This is due to the round particle shape and low specific surface; even if capillary surfaces may arise at lower suctions; the tensile forces in the meniscus are easier to break due to the relative large gap between particles.

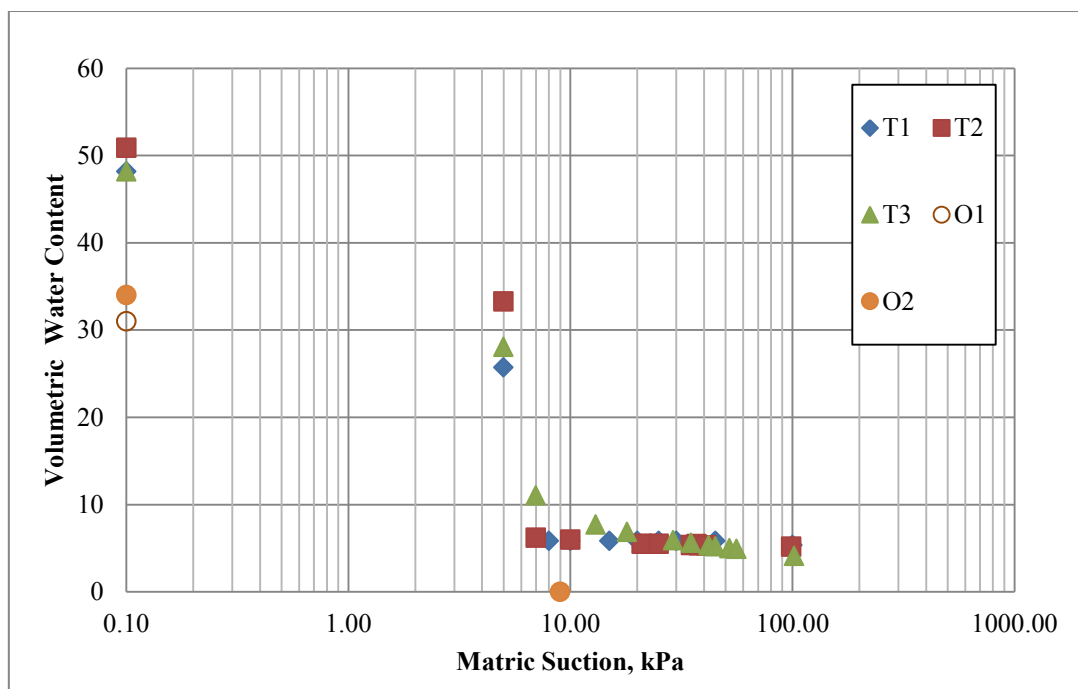


Figure 4.2: Raw test results for sand

4.2.4 Fitted Models

Table 4.3: Minimizing Sum of Square Error for Fredlund and Xing (1994) model

		θ	θ	$(\theta - \theta^*)^2$
Set T1	0.1	48.17	46.99	1.38
	5	25.71	28.37	7.05
	8	5.82	7.61	3.19
	10	5.82	6.52	0.5
	15	5.82	5.38	0.2
	20	5.82	4.84	0.96
	25	5.82	4.5	1.73
	30	5.82	4.27	2.41
	45	5.82	3.82	3.99
	100	5.34	3.16	4.77
				26.18
	Set T2	0.1	50.88	48.14
5		33.27	29.96	10.94
7		6.19	9.86	13.49
10		5.95	7.58	2.67
21		5.5	5.63	0.02
25		5.5	5.34	0.02
37		5.45	4.8	0.42
35		5.36	4.87	0.24
38		5.31	4.77	0.29
41		5.3	4.68	0.39
99		5.17	3.81	1.84
				37.82
Set T3	0.1	49.83	48.14	2.85
	5	29.14	29.96	0.68
	7	6.58	9.86	10.78
	13	6.11	6.69	0.34
	18	6.58	5.92	0.43
	29	6.58	5.12	2.12
	35	6.58	4.87	2.92
	42	6.58	4.65	3.72
	45	6.58	4.57	4.03
	52	6.03	4.41	2.61
	56	6.03	4.34	2.86
	102	6.11	3.79	5.39
			38.73	
		total sum=	102.73	

Table 4.4: Minimizing Sum of Square Error for Van Genuthcen (1980) model

	ψ	θ	θ^*	$(\theta^*-\theta)^2$
Set T1	0.10	48.17	49.62664	2.12
	5.00	25.71	29.37341	13.42
	8.00	5.82	5.955919	0.02
	10.00	5.82	5.874062	0.00
	15.00	5.82	5.869499	0.00
	20.00	5.82	5.869478	0.00
	25.00	5.82	5.869477	0.00
	30.00	5.82	5.869477	0.00
	45.00	5.82	5.869477	0.00
	100.00	5.34	5.869477	0.28
			sum =	15.86
Set T2	0.10	50.88	49.62664	1.57
	5.00	33.27	29.37341	15.18
	7.00	6.19	6.36864	0.03
	10.00	5.95	5.874062	0.01
	21.00	5.50	5.869478	0.14
	25.00	5.50	5.869477	0.14
	37.00	5.45	5.869477	0.18
	35.00	5.36	5.869477	0.26
	38.00	5.31	5.869477	0.31
	41.00	5.30	5.869477	0.32
	99.00	5.17	5.869477	0.49
		sum =	18.63	
Set T3	0.10	49.83	49.62664	0.04
	5.00	29.14	29.37341	0.05
	7.00	6.58	6.36864	0.04
	13.00	6.11	5.869622	0.06
	18.00	6.58	5.869479	0.50
	29.00	6.58	5.869477	0.50
	35.00	6.58	5.869477	0.50
	42.00	6.58	5.869477	0.50
	45.00	6.58	5.869477	0.50
	52.00	6.03	5.869477	0.03
	56.00	6.03	5.869477	0.03
	102.00	6.11	5.869477	0.06
		sum =	2.83	
		total sum =	37.32	

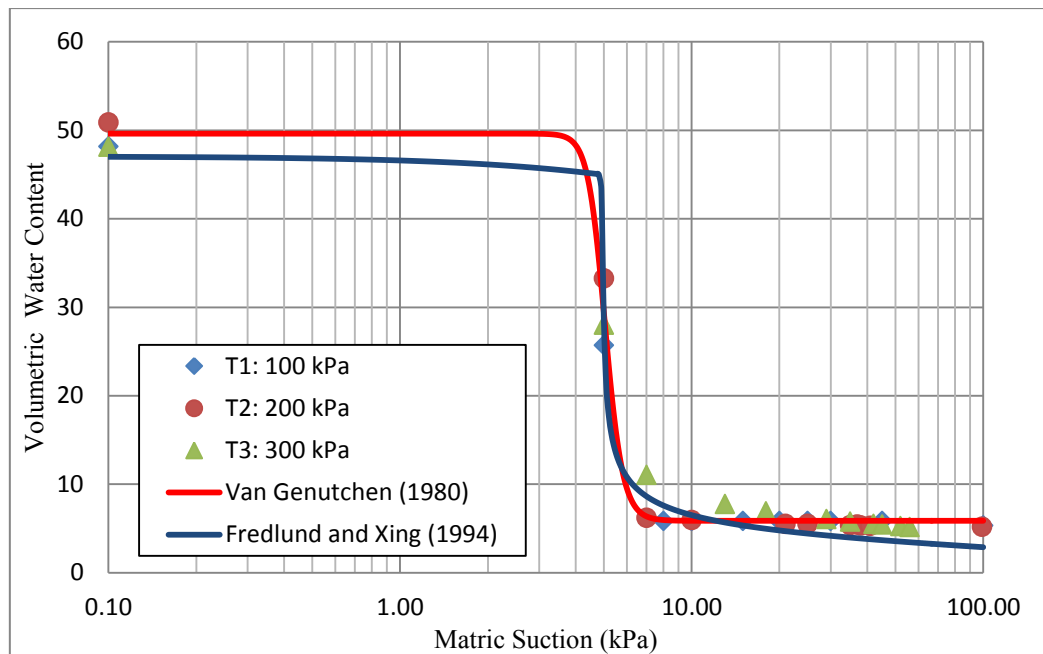


Figure 4.3: Modelling with FX and VG

After the use of parametric analysis to reduce the sum of square residuals (SSR), as shown in Table 4.3 and Table 4.4, the air-entry is approximated at 3 kPa. Figure 4.3 shows the fitted curve for Toyoura Sand for both model (1) and model (2). The summary of fitting parameters as follows:

Table 4.5: Summary of fitting parameters for Toyoura Sand

Fredlund & Xing (1994) model				
a	m	n	r	θ_s
4.9107	0.3671	220.702	26.615	49.6573
Van Genutchen (1980) model				
a	m	n	θ_r	θ_s
4.9851	0.8679	15.1716	5.870	49.6267

For this type of soil, the Van Genuthchen (1980) model tends to provide a better fit with a total SSE of 37.32 while Fredlund and Xing (1994) has a total sum of 102.73. It should be noted that the data for all pressure designs were taken collectively in the fitting since there is no significant difference in the data points for the three independent tests.

Based on Table 4.6, testing even under the *t-test*, there lies a significant difference in the variance of the models, stated as there is indeed a clarification that one model is different from the other. Both the one-tail and two-tail test rejects the *t-stat* value which implies rejection of the null hypothesis that there no difference of the two models.

Therefore; it is clear that the Van Genuchten (1980) can be concluded as a better fit for Toyoura Sand.

Table 4.6: Results of *t-test* for Toyoura Sand

	<i>Fredlund & Xing (1994)</i>	<i>Van Genuchten (1980)</i>
Mean	8.082	6.189
Variance	85.164	88.953
Observations	1000	1000
Pooled Variance	87.058	
Hypothesized Mean Difference	0	
<i>df</i>	1998	
t Stat	4.537	
P(T<=t) one-tail	3.01863E-06	
t Critical one-tail	1.646	
P(T<=t) two-tail	6.03725E-06	
t Critical two-tail	1.961	

4.2.5 Discussion of results

As shown in Figure 4.4, a study conducted by Rouf et. al. in 2012 using a unified measurement with suction control apparatus tended to produce the same sigmoidal shape and the values appear to juncture in the 5 kPa onwards. Therefore regardless of initial conditions, the values of suction will tend to be relatively close to each other only at higher suctions. Moreover, using different apparatuses may not lead to an identical SWCC; not only is the apparatus used is related for having non-identical SWCC but also the initial conditions, such as void ratio and compaction stress, are important factors that should be considered. It is evident though that the

SWCC has leaned towards the right; stated as the suctions are higher with the presence of confining pressure.

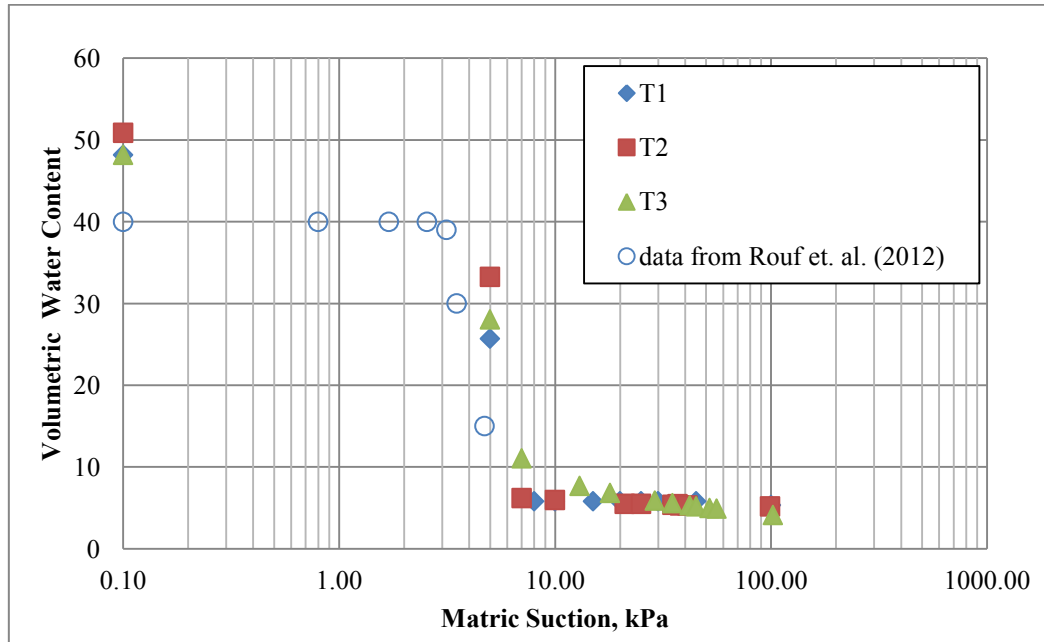


Figure 4.4: Suction values compared with existing work

4.3 SWCC of Khon Kaen Loess

4.3.1 Soil properties

The basic index properties of the soil sample are shown in Table 4.7 as well as the grain size distribution in Figure 4.5.

Table 4.7: Index Properties of Red Khon Kaen Loess

Khon Kaen Loess	<i>Punrattanasin (2002)</i>	<i>Nuntasarn (2011)</i>	<i>This Study (2013)</i>
Clay Content	5	13	8
Silt Content	30	31	25
Sand Content	65	56	67
Specific gravity	2.60	2.65	2.64
LL	16	20.3	20.61
PL	13	14.5	15.41
PI	3	5.8	5.20
USCS	SM	SM-SC	SM-SC
Optimum Moisture Content	9.7	8.25	-
Maximum Dry Density	2.11	2.00	-
Hydraulic Conductivity	2.8×10^{-6}	-	-

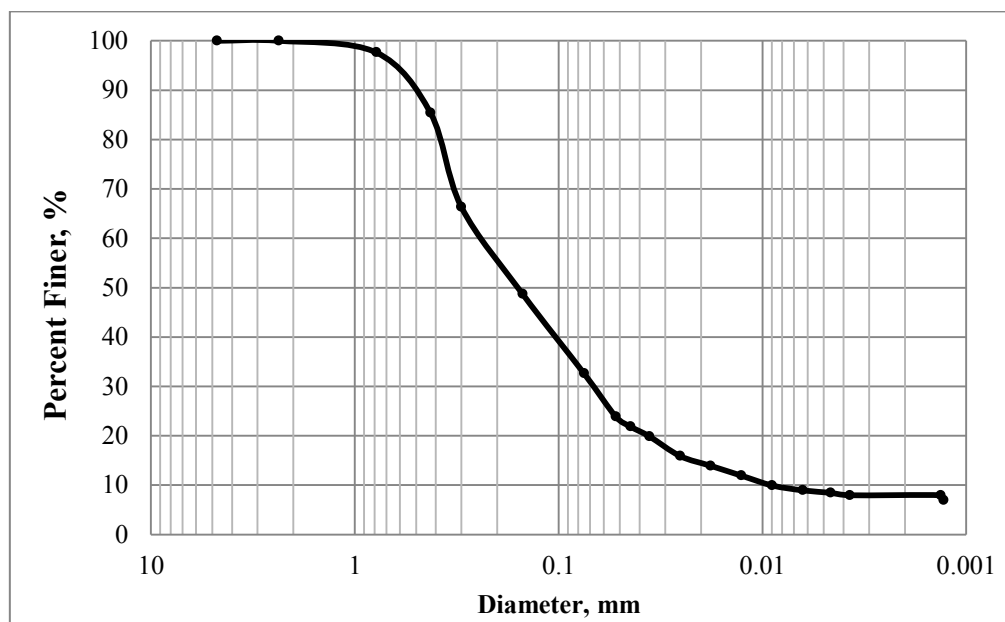


Figure 4.5: Grain Size Distribution of tested soil

The properties show that the soil specimen is classified as a mixture of Silty Clayed-Sand according to USCS standards. Numerous and repeated Atterberg tests have been done due to the peculiar behavior of the soil; there are instances that it behaves as a non-plastic material.

The mean size diameter d_{50} is at 0.160 mm. 29.3 Considerable amount of sand is present and 32.61% of the material passed the #200 sieve.

4.3.2 Matric suction from Unsaturated Triaxial Testing

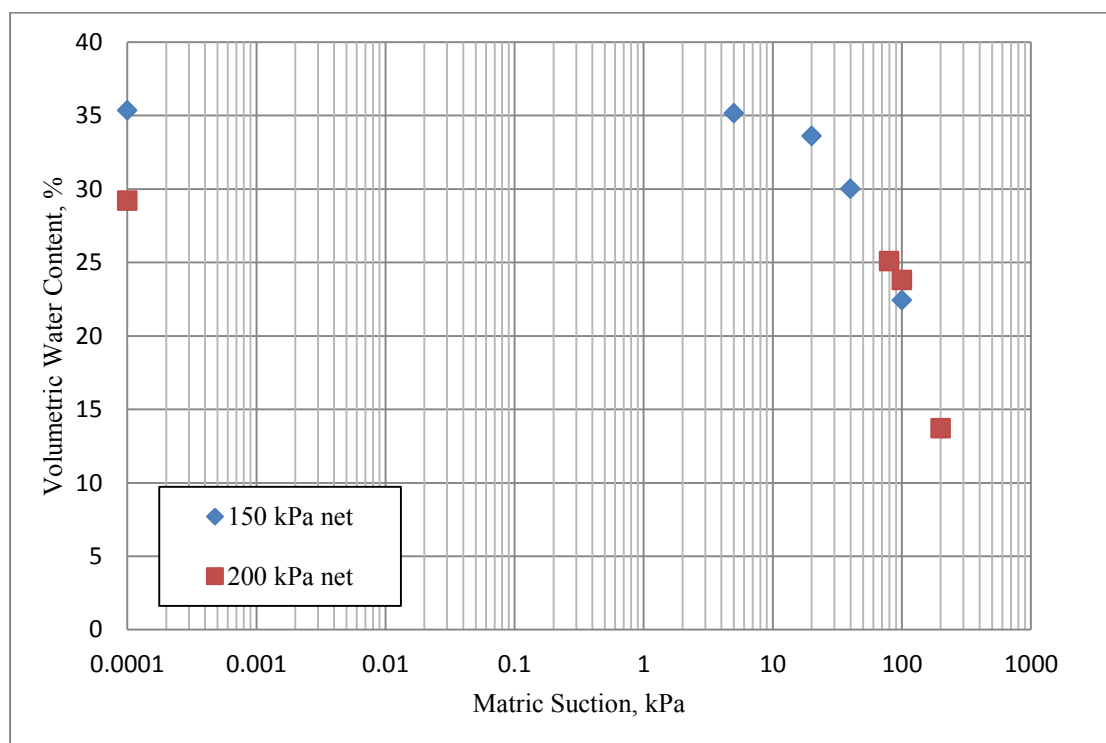


Figure 4.6: Plot of volumetric water content and suction of Khon Kaen Loess under a net confining stress of 150 kPa and 200 kPa

Experimental suction points of undisturbed loess from Unsaturated Triaxial testing are presented in Figure 4.6. The air-entry value for a net stress of 150 kPa is projected at approximately 20 kPa, and 35 kPa for a net stress of 200 kPa. The difference is possibly due to the initial void ratio and initial volumetric water content, as well as the higher confining pressure during testing.

4.3.3 Model Fitting for a net confining pressure of 150 kPa

Table 4.8: Minimizing Sum of Square Error for Fredlund and Xing (1994) model

	θ	θ^*	$(\theta-\theta^*)^2$
0.0001	35.341	35.341	0.000
5	35.151	35.186	0.001
20	33.602	33.527	0.006
0040	30.012	29.997	0.000
100	22.433	22.430	0.000
			0.007

Table 4.9: Minimizing Sum of Square Error for Van Genuchten (1980) model

	θ	θ^*	$(\theta-\theta^*)^2$
0.0001	35.341	35.341	0.000
5	35.151	35.279	0.017
20	33.602	33.673	0.005
40	30.012	29.859	0.023
100	22.433	22.752	0.102
			0.147

Table 4.10 Result of *t*-test for 150 kPa net confining stress test

	<i>Fredlund & Xing (1994)</i>	<i>Van Genuchten (1980)</i>
Mean	17.981	17.744
Variance	167.120	173.990
Observations	13	13
Pooled Variance	170.555	
Hypothesized Mean Difference	0	
df	24	
t Stat	0.046	
P(T<=t) one-tail	0.482	
t Critical one-tail	1.711	
P(T<=t) two-tail	0.963	
t Critical two-tail	2.064	

Table 4.8 and Table 4.9 shows the results of minimizing SSE for the 150 kPa net stress test. The target value for each total sum was 0.0 however; even if the target was not reached and the minimum values obtained were 0.007 and 0.147, it can still

be assumed that both curve-fitting models are suitable for the tested soil. This will be referred to as SWCC 1 for practical purposes.

From selected 13 points from the both models, including tested and additional 9 points were selected for verification. A *t*-test was then performed to verify if there is a significant difference between the two models; results are shown in Table 4.10. Both the one-tail and two-tail test indicate an acceptance of the null hypothesis that there is equal variance between the two. In other words, the two models, particularly the Fredlund & Xing (1994) and Van Genuchten (1980) fitting are suitable for the sample. The disadvantage to further confirm this, however is that there are no tested data points for suction beyond the 100 kPa in this test, therefore the values past this point are merely predicted potential values and must be confirmed by other test methods.

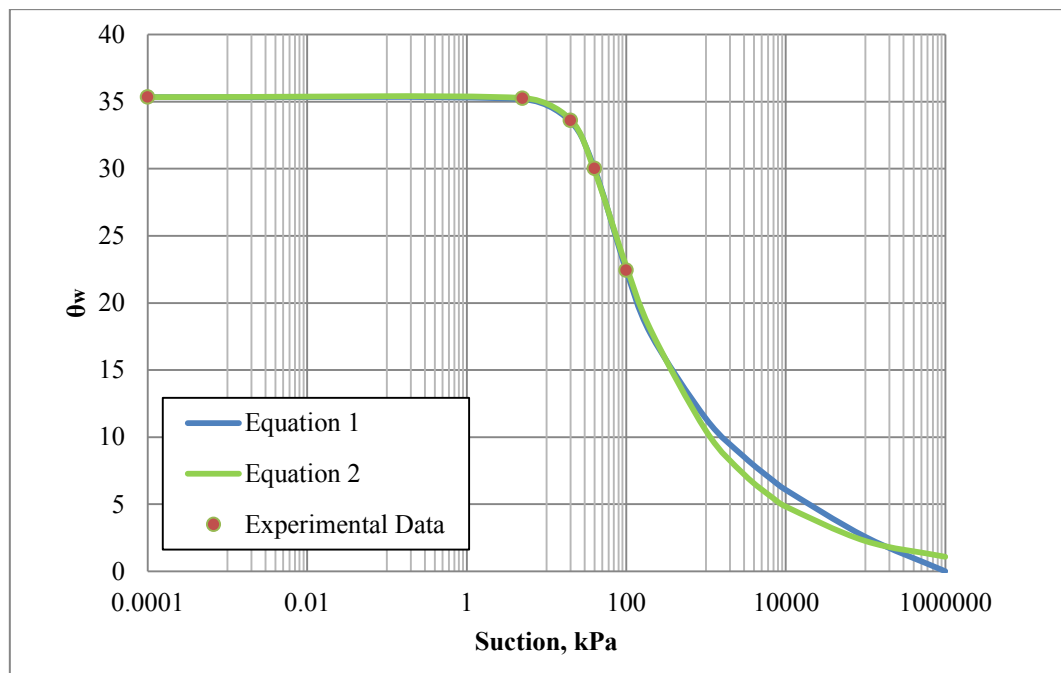


Figure 4.7: SWCC of Khon Kaen Loess under 150 kPa net stress

The summary of fitting parameters for Khon Kaen loess under a net stress of 150 kPa is listed in Table 4.11 and the final plot is illustrated in Figure 4.7.

Table 4.11: Summary of fitting parameters under a net stress of 150 kPa

Fredlund & Xing (1994) model				
a	m	n	r	θ_s
37.741	0.519	2.031	538.192	35.341
Van Genuchten (1980) model				
a	m	n	θ_r	θ_s
27.854	0.1349	2.5329	0.100	35.341

4.3.4 Model Fitting for a net confining pressure of 200 kPa

Table 4.12: Minimizing Sum of Square Error for Fredlund and Xing (1994) model

	θ	θ^*	$(\theta-\theta^*)^2$
0.0001	29.210	29.210	0.000
80	25.080	25.510	0.185
100	23.800	23.215	0.342
200	13.700	13.812	0.013
			0.540

Table 4.13: Minimizing Sum of Square Error for Van Genuchten (1980) model

	θ	θ^*	$(\theta-\theta^*)^2$
0.0001	29.210	29.210	0.000
80	25.080	25.720	0.409
100	23.800	23.226	0.330
200	13.700	13.843	0.020
			0.759

Table 4.12 and Table 4.13 show the results of minimizing SSE for the 200 kPa net stress test. Performing the procedure of minimizing the sum of squared errors with a target of 0.0, the values obtained were 0.540 and 0.759. The SSE was relatively higher than the previous curve fitting that may be related to the fewer number of points to be analysed.

Table 4.14 Result of *t-test* for 200 kPa net confining stress test

	<i>Fredlund & Xing</i> (1994)	<i>Van Genuchten</i> (1980)
Mean	14.717	14.243
Variance	164.287	179.833
Observations	13	13
Pooled Variance	172.060	
Hypothesized Mean Difference	0	
<i>df</i>	24	
t Stat	0.092	
P(T<=t) one-tail	0.464	
t Critical one-tail	1.711	
P(T<=t) two-tail	0.927	
t Critical two-tail	2.064	

Similarly, with 13 points each from both models, including tested and additional 9 points were selected for verification. A *t-test* was then performed to verify if there is a significant difference between the two models; results are shown in Table 4.14. Both the one-tail and two-tail test indicate an acceptance of the null hypothesis that there is equal variance between the two. To clarify this, the two models, particularly the Fredlund & Xing (1994) and Van Genuchten (1980) fitting are both suitable for the sample. The disadvantage to further confirm this, however is that there are no tested data points for suction beyond the 200 kPa in this test, therefore the values past this point are merely predicted potential values and must be confirmed by other test methods.

The summary of fitting parameters for Khon Kaen loess under a net stress of 200 kPa is listed in Table 4.15 and the final plot is shown in Figure 4.8 which will be referred to as SWCC 2 for practical purposes.

Table 4.15: Summary of fitting parameters under a net stress of 200 kPa

Fredlund & Xing (1994) model				
a	m	n	r	θ_s
104.490	0.8759	3.0115	1000.00	29.210
Van Genuchten (1980) model				
a	m	n	θ_r	θ_s
79.159	0.1717	4.4015	0.100	29.210

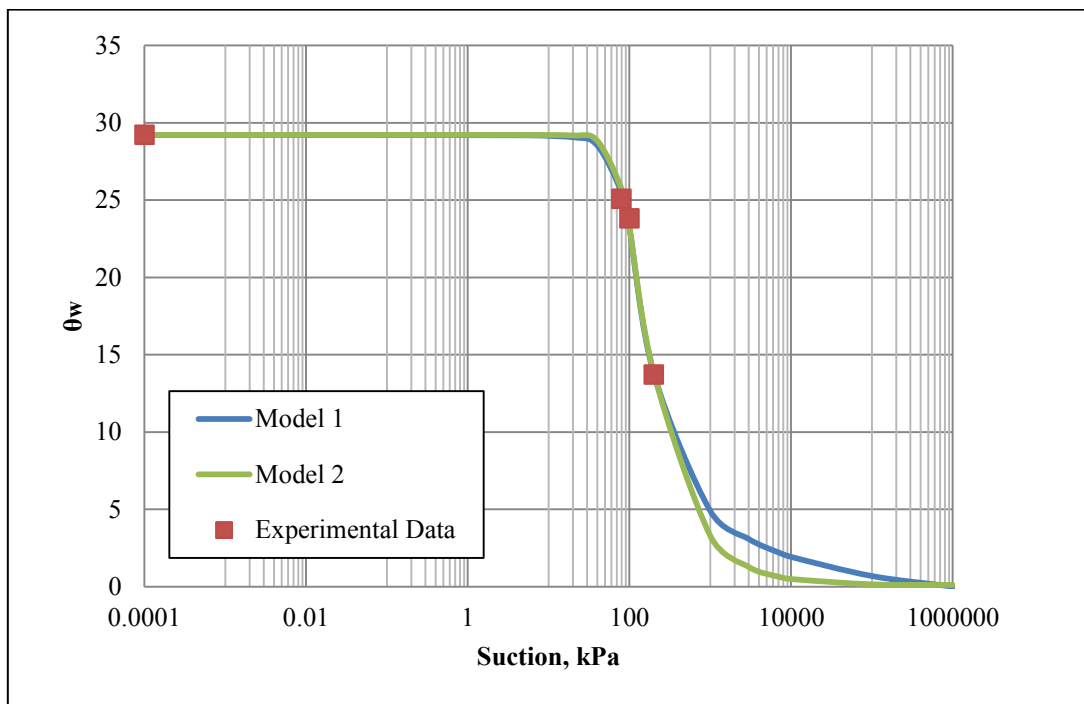


Figure 4.8: SWCC of Khon Kaen Loess under 200 kPa net stress

4.3.5 Comparison with existing models

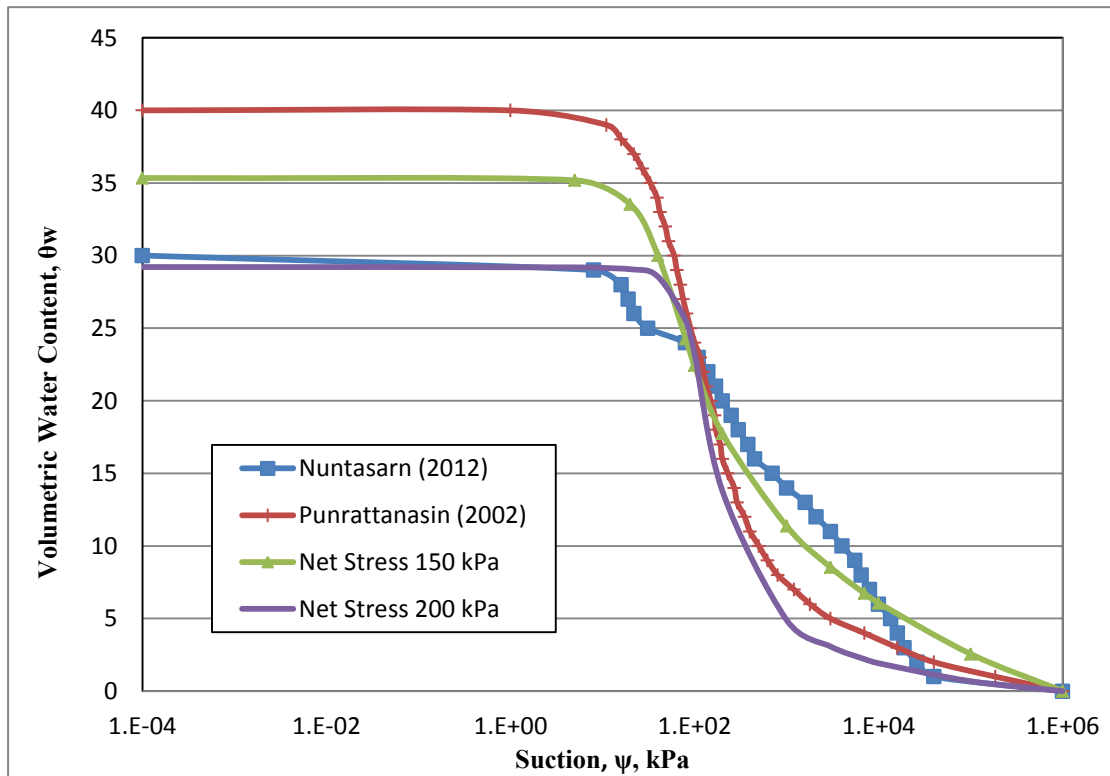


Figure 4.9: SWCC comparisons with existing works

Based on the two SWCCs produced by unsaturated triaxial conditions, the starting point of the lower net stress has higher initial volumetric water content. This is due to the higher initial void ratio and also due to the consolidation process for the second test.

SWCC from compacted soil and undisturbed conditions are exhibited in Figure 4.9. A compacted soil produced a steeper sloped curve starting from a volumetric water content of 40% leaning to the left as the residual state started at a much lower value and produced a reduced transition range 25kPa to 500kPa (Punrattanasin et.al, 2011).

In comparison with the prepared sample starting at 30% volumetric water content by Nuntasarn (2011), a lower air-entry value of 12kPa and a higher residual state was achieved at 45,000 kPa. The shape of this curve may suggest that the soil

may have a dual-porosity curve, meaning there is a possibility that the *real* SWCC may be a series of curves, however, no experimental data has been produced as evidence.

Finally, this translates that SWCC is dependent on sample preparation, initial conditions and methods of testing. No particular single curve can exist even for the same soil but caution must be exercised for the application for other purposes.

4.3.6 Unified Khon Kaen SWCC

To avoid bias in the estimation of unsaturated shear strength, the SWCC to be use must be unified. In order to achieve this, suction points were derived from average of the two previous curves and the SSE was applied for models 1 and 2. Figure 4.10 and Table 4.16 show the prediction of the median curve.

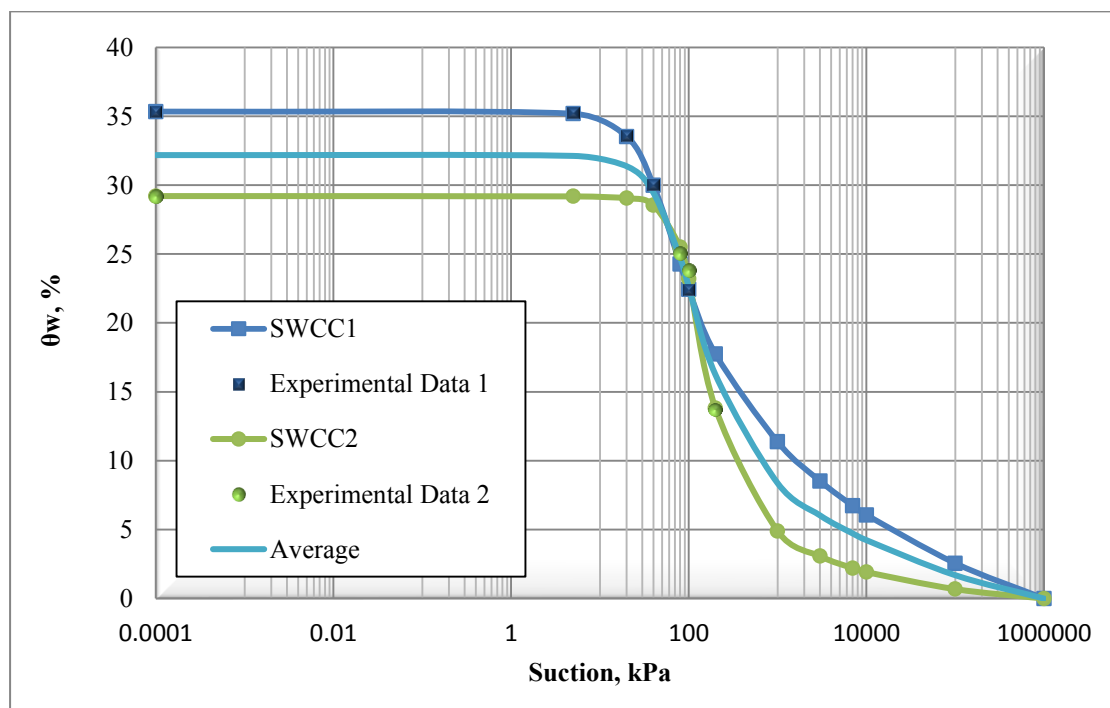


Figure 4.10: Average curve for tested and fitted

Table 4.16: Prediction of Median SWCC using Fredlund and Xing (1994)

	θ	θ^*	$(\theta-\theta^*)^2$
0.0001	32.275	32.189	0.007
5	32.187	32.128	0.004
20	31.295	31.379	0.007
40	29.268	29.447	0.032
80	24.891	24.724	0.028
100	22.822	22.640	0.033
200	15.776	16.238	0.214
1000	8.134	8.378	0.059
3000	5.803	6.036	0.054
7000	4.474	4.727	0.064
10000	3.993	4.240	0.061
100000	1.621	1.696	0.006
1000000	0.000	0.000	0.000
			0.569

Table 4.17 Prediction of Median SWCC using Van Genuchten (1980)

	θ	θ^*	$(\theta-\theta^*)^2$
0.0001	32.275	32.189	0.007
5	32.187	32.176	0.000
20	31.295	31.655	0.130
40	29.268	29.480	0.045
80	24.891	24.306	0.342
100	22.822	22.371	0.203
200	15.776	16.886	1.231
1000	8.134	8.613	0.230
3000	5.803	5.491	0.097
7000	4.474	3.918	0.309
10000	3.993	3.410	0.340
100000	1.621	1.492	0.016
1000000	0.000	0.785	0.617
			3.567

In Table 4.16, a sum of square error (SSE) of 0.569 was obtained for the study of the median curve, where the largest errors are in the suction range of 40 kPa to 100,000 kPa. Likewise in Table 4.17, but a larger SSE was obtained at 3.567.

Table 4.18 Results of *t*-test for the average Khon Kaen SWCC

	<i>Fredlund & Xing</i> (1994)	<i>Van Genuchten</i> (1980)
Mean	16.448	16.367
Variance	161.712	164.215
Observations	13	13
Pooled Variance	162.963	
Hypothesized Mean Difference	0	
<i>df</i>	24	
t Stat	0.016	
P(T<=t) one-tail	0.494	
t Critical one-tail	1.711	
P(T<=t) two-tail	0.987	
t Critical two-tail	2.064	

Table 4.19: Summary of fitting parameters for the median SWCC

Fredlund & Xing (1994) model				
<i>a</i>	<i>m</i>	<i>n</i>	<i>r</i>	θ_s
70.523	0.802	1.939	5980.02	32.189
Van Genuchten (1980) model				
<i>a</i>	<i>m</i>	<i>n</i>	θ_r	θ_s
44.299	0.158	2.742	0.373	32.189

There is no significant difference in fitted SWCC for both models as shown in Table 4.18. The fitting parameters are summarized in Table 4.19. It is notable that the computed residual suction is considerably higher than the two previous curves, suggesting a wider range of transition range.

The final SWCC for Khon Kaen Loess is plotted in Figure 4.11 with a saturated water content of 32.189, residual water content of approximately 6.20, and an air-entry value of 30 kPa.

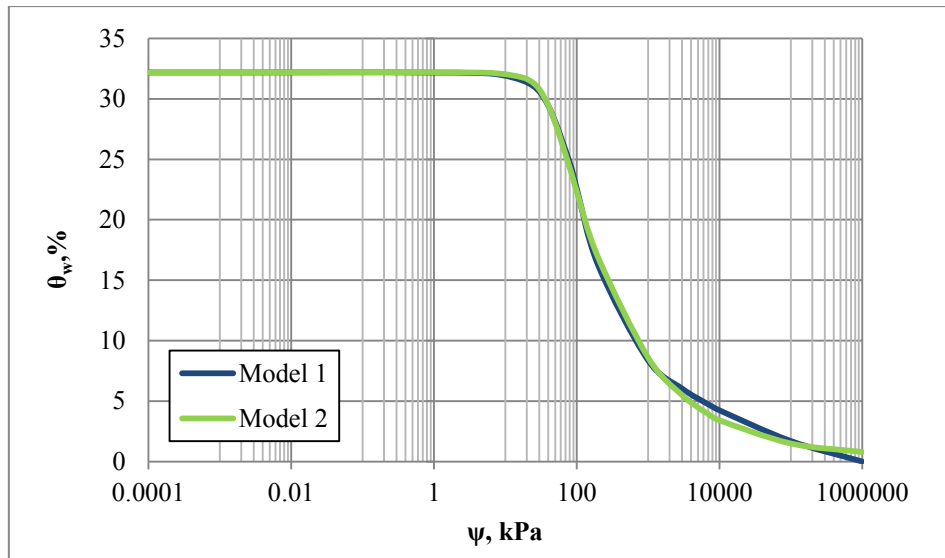


Figure 4.11: Khon Kaen SWCC

4.4 Analysis of Khon Kaen Data

37 test results for Unconsolidated Undrained triaxial tests (UU) for soil samples obtained from a depth of 2.0 to 4.0 meters. These were from Dr. Watcharin Gasaluck of Khon Kaen University, which are given in Table 4.20. Majority were classified as Silty Sand and Clayey Sand. The normal stresses were calculated from the dry unit weight, while the volumetric water content was derived from the volume-mass relationships such as void ratio from the data. These were used to project the corresponding suction from the tested SWCC. By using equation (13) suggested by Fredlund et. al. (1978) under the extended Mohr-Coulomb failure criterion whose unsaturated parameters are aimed to be established.

Table 4.20: Khon Kaen properties and parameters

No.	Location	Depth, m	USCS	G_s	γ_{dry} , kN/m ³	S, %	c, kPa	ϕ , °	w, %	e	θ_w		σ	χ	τ_{unsat}
1	Khon Kaen	2	SC	2.62	18.10	89.03	13.83	8.07	14.19	0.42	26.23	64.14	36.20	0.66	24.95
2	Khon Kaen	2	SC	2.62	17.69	82.52	35.48	5.12	14.16	0.45	25.59	70.45	35.38	0.63	42.60
3	Khon Kaen	2	SC	2.62	17.78	76.86	46.28	5.16	13.13	0.45	23.76	88.70	35.56	0.55	53.90
4	Khon Kaen	3	SM	2.68	16.05	34.21	25.95	24.19	8.01	0.63	13.19	373.33	48.15	0.25	89.49
5	Khon Kaen	3	SM	2.68	15.85	25.96	38.47	32.79	6.27	0.65	10.20	688.58	47.55	0.18	148.27
6	Khon Kaen	2.5	SM-SC	2.71	15.66	42.81	68.50	28.70	11.02	0.70	17.59	172.77	39.15	0.38	126.05
7	Khon Kaen	2.5	SM-SC	2.71	15.51	41.67	70.18	29.04	10.98	0.71	17.36	177.13	38.78	0.38	128.74
8	Khon Kaen	3	SM	2.67	15.39	19.08	79.68	34.44	4.97	0.70	7.83	1293.02	46.17	0.13	223.23
9	Khon Kaen	2	SM	2.67	15.12	72.92	19.62	24.70	20.00	0.73	30.83	24.35	30.24	1.12	46.09
10	Khon Kaen	2	SM	2.63	13.95	43.90	15.86	29.68	13.38	0.80	19.53	140.04	27.90	0.43	65.97
11	Khon Kaen	2	SM	2.63	14.71	40.33	10.13	32.62	11.56	0.75	17.33	177.70	29.42	0.38	71.71
12	Khon Kaen	2	SM	2.64	15.40	45.97	21.91	20.81	11.87	0.68	18.63	154.37	30.80	0.41	57.45
13	Khon Kaen	2	SM	2.64	14.51	40.36	19.94	22.78	12.00	0.78	17.75	169.80	29.02	0.39	59.61
14	Khon Kaen	2	SM	2.68	14.88	46.13	3.92	26.57	13.20	0.77	20.02	132.80	29.76	0.44	48.11

No.	Location	Depth, m	USCS	G_s	γ_{dry} , kN/m ³	S_v , %	c , kPa	ϕ , °	w , %	e	θ_w		σ	χ	τ_{unsat}
15	Khon Kaen	2	SM	2.68	13.38	33.86	11.94	28.81	10.19	0.81	15.12	251.46	26.76	0.31	69.61
16	Khon Kaen	2	SM	2.65	14.97	48.79	3.92	30.96	13.56	0.74	20.69	123.51	29.94	0.46	55.90
17	Khon Kaen	2	SM	2.65	14.99	56.37	0.00	31.19	15.62	0.73	23.87	87.66	29.98	0.55	47.57
18	Khon Kaen	2	SM	2.65	15.05	50.39	0.00	32.68	13.83	0.73	21.22	116.62	30.10	0.47	54.76
19	Khon Kaen	2	SM	2.62	14.39	24.96	3.27	37.60	7.49	0.79	10.99	585.75	28.78	0.20	113.42
20	Khon Kaen	2	SM	2.61	14.83	37.65	9.15	31.80	10.48	0.73	15.84	217.00	29.66	0.34	72.85
21	Khon Kaen	2	SM	2.61	14.81	38.78	19.94	26.57	10.83	0.73	16.35	197.60	29.62	0.35	69.79
22	Khon Kaen	2	SM	2.61	14.02	34.08	2.29	34.99	10.79	0.83	15.42	236.48	28.04	0.32	75.09
23	Sakolnakorn	2.5	SM	2.69	17.34	81.13	2.34	21.90	15.73	0.52	27.81	50.86	43.36	0.75	35.06
24	Sakolnakorn	2.5	SC	2.66	16.82	84.39	4.46	20.10	17.49	0.55	29.99	32.92	42.06	0.95	31.30
25	Sakolnakorn	2.5	SC	2.61	16.71	84.47	1.10	16.20	17.24	0.53	29.36	40.51	41.76	0.85	23.21
26	Korat	2	SC	2.71	15.99	55.18	81.12	19.10	13.50	0.66	22.00	107.17	31.98	0.50	110.62
27	Korat	3.5	SC	2.72	15.98	40.84	69.63	24.80	10.05	0.67	16.38	196.96	55.93	0.36	127.80
28	Korat	3	SM	2.7	16.95	35.04	35.06	38.70	7.30	0.56	12.61	420.40	50.85	0.23	154.64
29	Nongkai	2	SC	2.69	17.06	24.12	42.31	41.20	4.90	0.55	8.52	971.27	34.12	0.15	197.77

No.	Location	Depth, m	USCS	G_s	γ_{dry} , kN/m ³	S, %	c, kPa	ϕ , °	w, %	e	θ_w		σ	χ	τ_{unsat}
30	Nongkai	2	SC	2.69	16.90	36.84	48.33	34.71	7.69	0.56	13.25	368.77	33.80	0.25	136.01
31	Nongkai	2	SC	2.69	17.13	48.19	62.73	23.98	9.68	0.54	16.90	186.17	34.26	0.37	108.32
32	Nongkai	1.5	ML	2.68	15.42	28.76	22.94	32.15	7.56	0.70	11.89	487.17	23.13	0.22	103.57
33	Nongkai	4	SC	2.7	18.08	64.18	47.45	15.12	11.05	0.46	20.37	127.86	72.32	0.45	82.55
34	Nongkai	3.5	SC	2.66	17.30	77.99	62.58	9.55	14.90	0.51	26.28	63.67	60.55	0.66	79.84
35	Kalsin	3	ML	2.65	15.89	26.57	35.81	41.12	6.38	0.64	10.33	670.50	47.67	0.18	183.42
36	Chaiyabhum	3	SM	2.71	15.61	23.20	32.66	40.81	6.02	0.70	9.58	781.78	46.83	0.17	185.44
37	Chaiyabhum	3	SM	2.71	15.50	37.17	43.69	16.13	9.81	0.72	15.50	232.64	46.50	0.32	78.95

4.4.1 Unsaturated shear strength

To be able to generate the surface of failure, a multiple regression analysis was applied among three variables: normal stress, suction and unsaturated shear strength. The first two variables were held as independent while the shear strength was the dependent variable. Under a confidence interval of 95%, a correlation R^2 of 0.789 was obtained using the 37 data points. Statistics are listed in Table 4.21 and Table 4.22.

Table 4.21: Regression Statistics

Multiple R	0.888
R Squared	0.789
Adjusted R Square	0.777
Standard Error	24.090
Observations	37

Table 4.22: Analysis of Variance

	<i>df</i>	<i>SS</i>	<i>MS</i>	<i>F</i>	<i>Significance F</i>
Regression	2	73914.38	36957.191	63.680	3.181 E-12
Residual	34	19732.03	580.354		
Total	36	93646.42			

The degree of freedoms was plotted in the statistics table from the Appendix with a F_0 of 3.26, and since the F-stat for the test is 63.68 which is greater than the F_0 value, we accept that there the test is significant and can be accepted. The coefficients are given in Table 4.23.

Table 4.23: Coefficient table

	Coefficients	Standard Error	P-value
Intercept	16.40	14.87	0.278
	0.15	0.01	2.41E-12
σ	0.87	0.38	0.027

4.4.2 Fitted model and unsaturated parameters

Applying linearization of unsaturated shear strength with respect to both the normal stress and matric suction as independent variables will yield to the extended Mohr-Coloumb criteria as plotted in Figure 4.12.

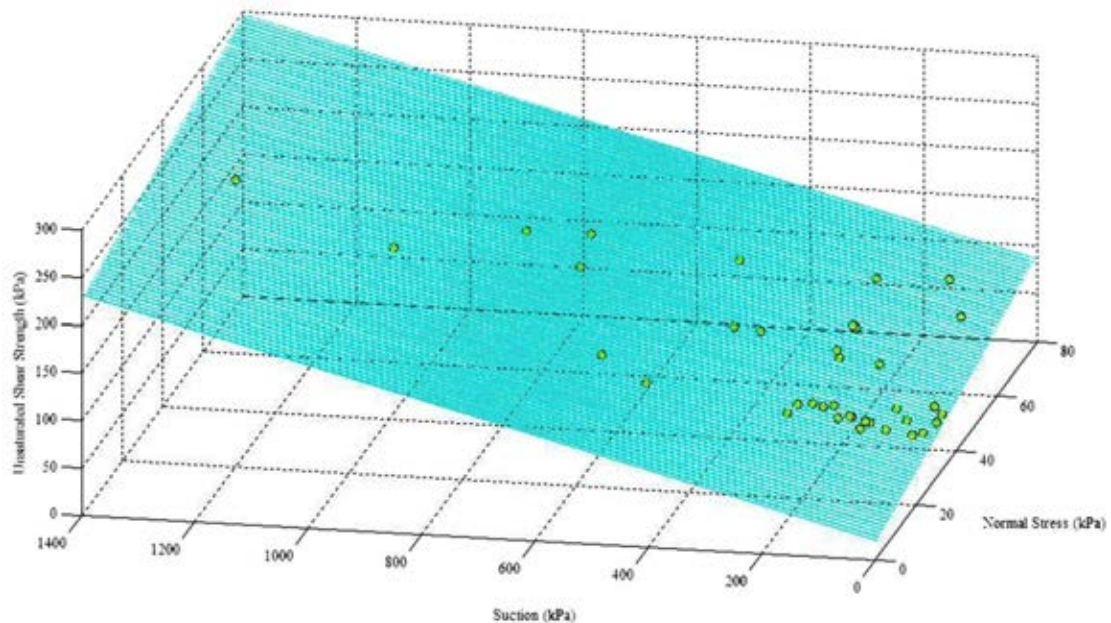


Figure 4.12: Unsaturated shear strength plane

The established SWCC encompasses a wide range of transition zone between the air-entry and residual suctions, the calculated angle of internal friction with respect to suction is 8° , which is in the acceptable range of values. The total cohesion intercept of 16.40, which is a combined effect of cohesion and cohesion with respect to suction. The angle of internal friction is calculated at 32° which is reasonable since the average of all tested angles is 26.35° .

4.5 Comparison with existing works

In comparison with the work on unsaturated silty sand by Schnellmann et. al (2013) with an average effective angle of friction of 34.7° and varying total cohesion intercept of 3 to 31 kPa, our results seem to be in the appropriate range and hence, acceptable.

4.6 Shear testing under triaxial conditions

This section presents the shear tests performed on the samples under UU and CU test. Two types of stress parameters were used: 2D plane strain condition and triaxial axi-symmetry condition. The first state is defined by:

$$s' = \frac{1}{2}(\sigma'_1 + \sigma'_3) \quad (25)$$

$$t = \frac{1}{2}(\sigma'_1 - \sigma'_3) \quad (26)$$

The second state is defined by:

$$p' = \frac{1}{3}(\sigma'_1 + 2\sigma'_3) \quad (27)$$

$$q = (\sigma'_1 - \sigma'_3) \quad (28)$$

The σ_1 and σ_3 are the axial stress and radial stresses, respectively applied in the vertical and horizontal plane. During the isotropic consolidation stage, the axial and radial stresses are equal in magnitude; the shear phase is where the vertical load is increased at a fixed rate until such time that the specimen reaches failure.

4.5.1 Unconsolidated Undrained Test

The sample was tested in an undisturbed condition, with the use of Unconsolidated Undrained (UU) testing with a confining pressure of 200 kPa applied with an axial strain rate of 0.1% per minute, however, the failure was not reached due to the maximum limit of axial displacement of the equipment which is 25mm. No sign

of shear failure was observed as shown in Figure 4.13. The comparison of the sheared sample under the UU testing produced a radial strain of 5.71% and a volumetric strain of 6.85% as seen in Figure 4.14. It is expected that the failure plane is in the vertical axis, similar to a CU tested sample under a net stress of 200 kPa as shown in Figure 4.18 which is indication that the sample has a brittle nature. Figure 4.15 and Figure 4.16 shows the results in both paths of stresses in the $s' vs t$ and $p' vs q$.



Figure 4.13: Sample after UU test



Figure 4.14: Comparison of sheared sample with the original size

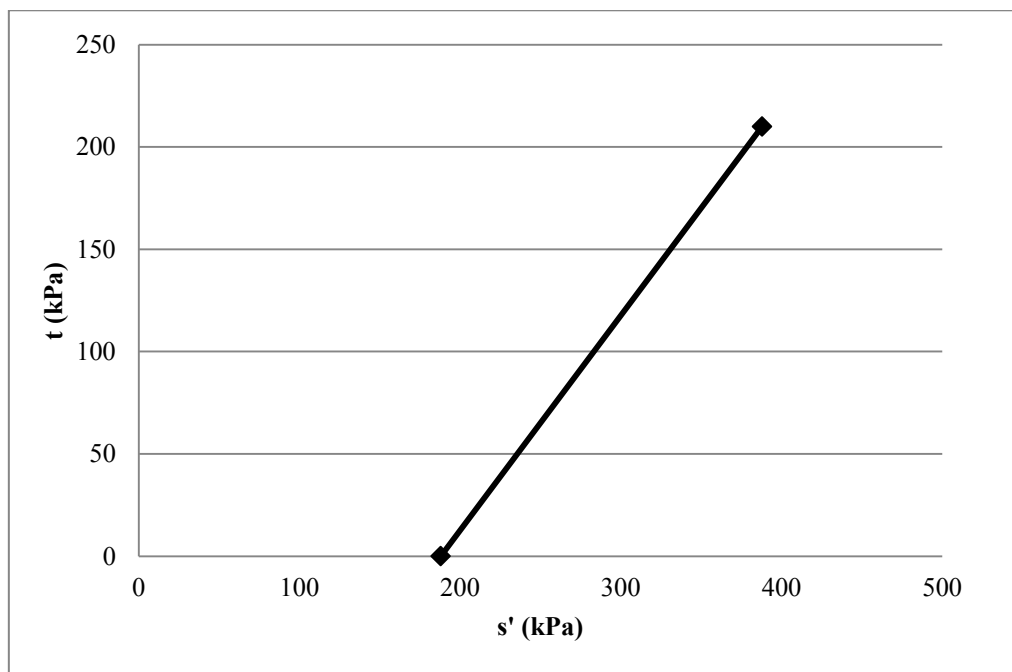


Figure 4.15: Shear path along the s' and t in UU testing

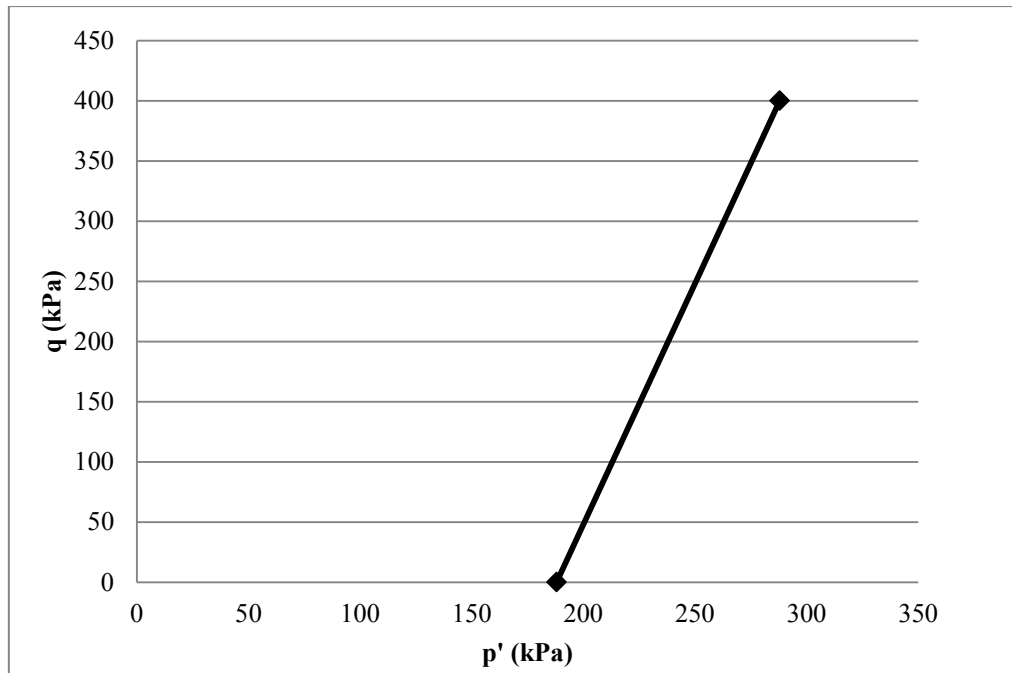


Figure 4.16: Shear path of p' and q in UU testing

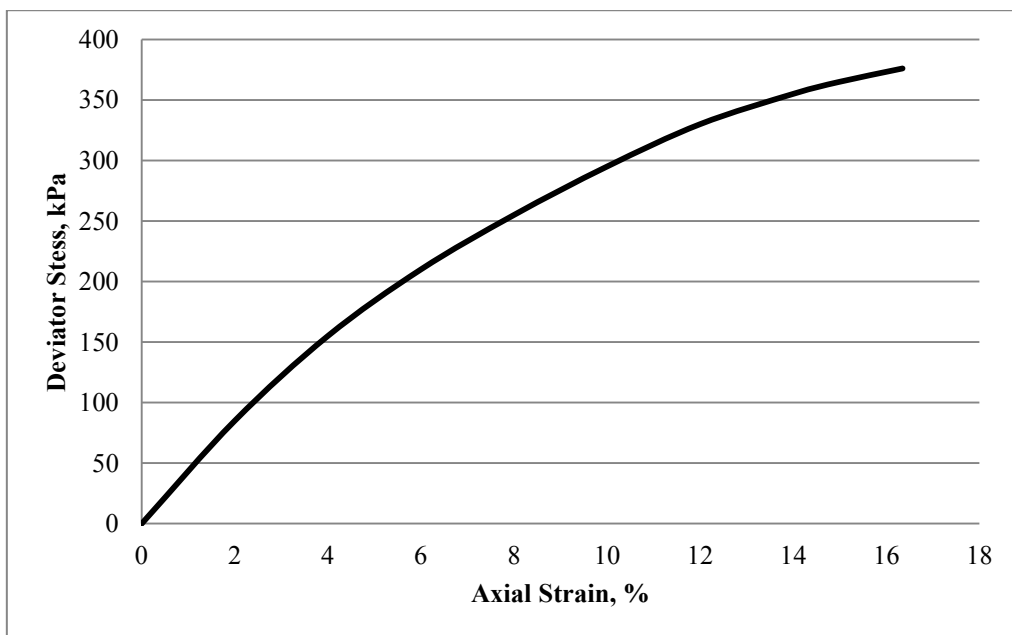


Figure 4.17 Axial Strain vs. Deviator Stress

It can be seen in Figure 4.17 that no failure was reached as the specimen did not attain a peak deviator stress and is confirmed by Figure 4.13.

4.5.2 Consolidated Undrained Test

The specimen subjected to a 450 kPa cell pressure and 250 kPa back pressure was applied with an axial strain rate of 0.5%. The axial strain at failure was observed at 9% with a corresponding deviator stress of 98 kPa. The results of the triaxial testing under CU conditions are shown in Figures 4.18 to 4.20. A volumetric strain of 4.34% was undertaken during the shear stage.



Figure 4.18: Shear failure on a CU test

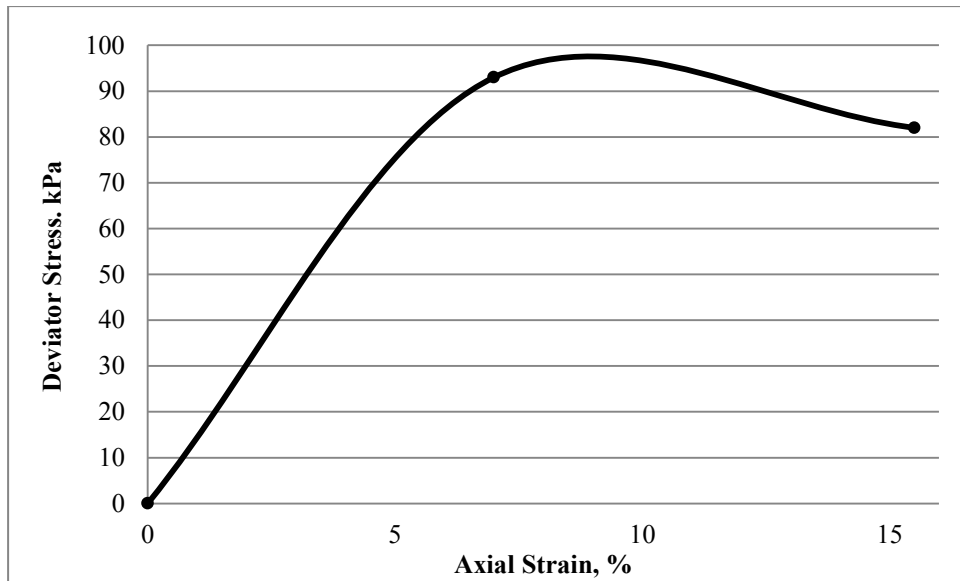


Figure 4.19 Axial Strain vs. Deviator Stress in a CU test

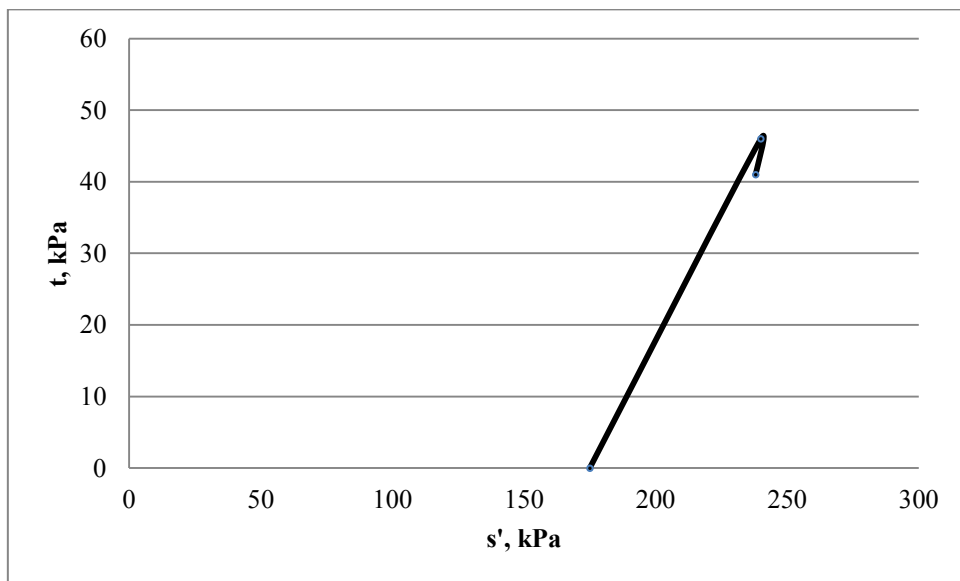


Figure 4.20 Stress path of s' vs t in a CU test

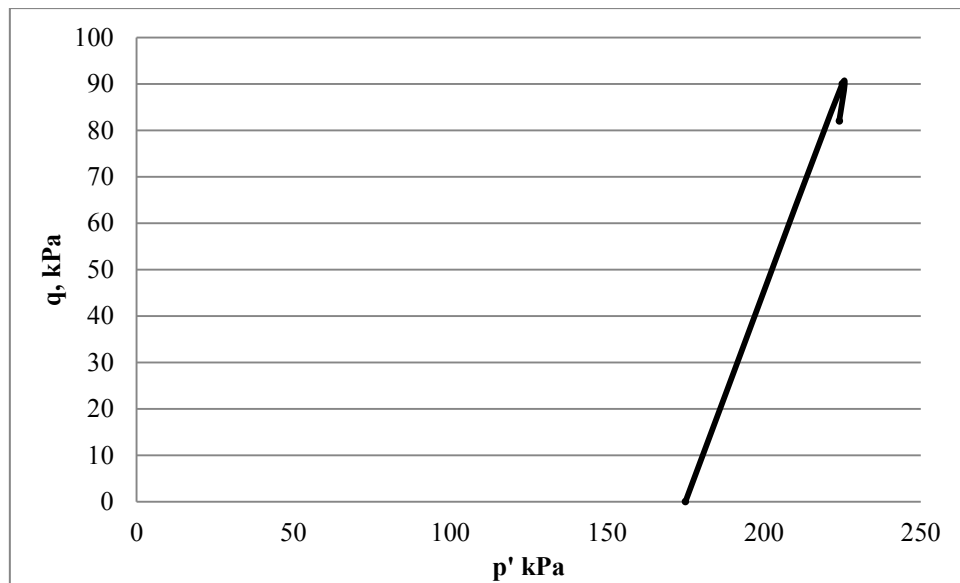


Figure 4.21 Shear path of p' vs q in a CU test

It can be seen that the shear failure is significantly lower in the CU test; since it was performed subsequent to the application of air pressure for the production of the SWCC, there is a possibility that the soil structure was changed during the process. It was subjected to a prior 7-day period of saturation, consolidation and Soil-Water stage; therefore, it is recommended that a separate test be done on the sample to avoid possible disturbance on the soil structure and fabric. To clarify this point, when the specimen is subjected to high air pressures, even with the application of confining pressure, there lies a possibility that the plane of shear failure from the top may have sprung from a preferential flow path owed to the application of air pressure.

CHAPTER V

CONCLUSION AND RECOMMENDATION

5.1 Conclusion

Based on the results, the following conclusions may be derived:

SANDS:

1. With the use of an unsaturated triaxial apparatus, the soil water curve for Ottawa Sand cannot be perceived due to the pressure limits of the machine. Ottawa sand having a mean size diameter of 0.835 mm, together with rounded and smooth surface will not sustain water with an initial applied suction of 5kPa.
2. Toyoura sand, with a mean size diameter of 0.210 and a bigger specific surface was established to have an air-entry value of 3 kPa and a residual suction of approximately 6 kPa.
3. The Van Genuchten (1980) curve model for SWCC was the best fitting model for the tested data points for Toyoura Sand solely based on the least sum of square residual; which is confirmed with the use of *t-test*, where there is a significant difference between the two models.

The main purpose of this research is to observe the suction that exists in Khon Kaen Loess and from the laboratory measurements and fitting of the SWCC, this was accomplished.

LOESS:

1. The experimental suction using an unsaturated triaxial system was applied until 200 kPa, with net stresses of 150 and 200 kPa.
2. SWCC fitting was best fitted by the Fredlund and Xing (1994) with the aid of sum of squared residuals (SSR); on the other hand the *t-test* implies that no significant difference exists between the results obtained for the two models.

3. The air-entry value is projected at 30 kPa.
4. On the analysis of 37 data sets of North-eastern Thailand soils, with respect to a 3D plane coupled with statistics, the following unsaturated shear strength parameters may be derived: a total cohesion of 16.394 kPa with a ϕ of 32° and an angle of internal friction with respect to suction ϕ_b of 8° .

5.2 Recommendations

One of the main advantages of using the experimental system is given by the presence of confining pressure and water pressure, which, if used correctly may closely model *in-situ* stress. Moreover, the flow measurements are given in *real-time* conditions, such that close monitoring of equilibrium of pressure and flow measurements can be examined.

SANDS:

1. The utilized apparatus is not the best suitable device to observe suction and water content change for the tested sands, having relatively larger grain sizes, is more appropriate to be tested with apparatuses that can sustain suctions in 0.1 kPa increments.

LOESS:

1. Perform further tests with a wider range of suction is recommended, more data points will provide a more accurate curve fitting.
2. Measurement of *in-situ* suction that may help estimate the real suction that exists in a soil needs to be studied further.
3. Proper caution should be observed when estimating the limits of suction that may exist in the soil, particularly the air-entry and residual suction values.
4. The unsaturated shear is extremely sensitive to the suction values, therefore proper measurement and estimation should be exercised.

REFERENCES

- American Society for Testing and Materials Standards. **ASTM Standard Test Methods for Determination of the Soil Water Characteristic Curve for Desorption Using a Hanging Column, Pressure Extractor, Chilled Mirror Hygrometer, and/or Centrifuge: ASTM D6836-02**. Philadelphia: ASTM Committee on Standards, 2003.
- Fetter, C.W. **Contaminant Hydrogeology**. New Jersey: Prentice Hall, 1999.
- Fredlund, D.G. and Rahardjo, H. **Soil Mechanics for Unsaturated Soils**. New York: John Wiley & Sons, 1993.
- Fredlund, D.G. and Xing A. Equations for the soil-water characteristic curve. **Canadian Geotechnical Journal** 31 (1994): 521-532.
- Fredlund, D.G. Sheng, and D. Zhao, J. Estimation of soil suction from the soil-water characteristic curve. **Canadian Geotechnical Journal** 48 (2010): 186-198.
- Fredlund, D.G., Xing A., Fredlund, M.D., and Barbour, S.L. The Relationship of the Soil Shear Strength Functions to the soil-water characteristic curve. **Canadian Geotechnical Journal** 3 (1995): 400-448.
- Fredlund, D.G. Use of soil-water characteristic curve in the implementation of unsaturated soil mechanics. **Proceedings of the Third International Conference in Unsaturated Soils**, Recife, Brazil, March 2002.
- Guan, G., Rahardjo, H., and Choon, L. Shear Strength Equations for Unsaturated Soil under Drying and Wetting. **ASCE Journal of Geotechnical and Geoenvironmental Engineering** 136(4) (2010): 594–606.
- Houston, S. L. Applied Unsaturated Soil Mechanics. **Proceedings of the Third International Conference in Unsaturated Soils**, Recife, Brazil, March 2002.
- Indrawan, I.G.B, Rahardjo, H. and Leong, E.C. Effects of coarse-grained materials on properties of residual soil. **Engineering Geology** 82 (2006): 154–164.
- Khalili, N., and Khabbaz, M. H. A unique relationship for χ for the determination of shear strength of unsaturated soils. **Geotechnique** 48(5) (1998): 681-687.

- Lee, I.-M., Sung, S.-G., and Cho, G. C. Effect of stress state on the unsaturated shear strength of a weathered granite. **Canadian Geotechnical Journal** 42(2) (2005): 624-631.
- Lu, N. and Likos, W. J. **Unsaturated Soil Mechanics**. New York: John Wiley & Sons, 2004.
- Mairaing, W. Jotisankasa, A., and Soralump, S. Some applications of unsaturated soil mechanics in Thailand: an appropriate technology approach. **Proceedings of the 5th Asia Pacific Conference on Unsaturated Soils**, 45-58. Pattaya, Thailand, 2011.
- Montgomery D.C. and Runger, C.R. **Applied Statistics and Probability for Engineers**. John Wiley & Sons, 2003.
- Nam, S. Gutierrez, M. Panayiotis, D. Petrie, J. Wayllace, A. Lu, N and Munoz, JJ. Comparison of testing techniques and models for establishing the SWCC of riverbank soils. **Engineering Geology** (2009): 1-10.
- Ng, C.W. and Bruze Menzies. **Advanced Unsaturated Soil Mechanics and Engineering**. Taylor and Francis, 2007.
- Nuntasarn, R. The undrained shear strengths of unsaturated khon kaen loess. **Proceedings of the 5th Asia Pacific Conference on Unsaturated Soils**, 197-202. Pattaya, Thailand, 2011.
- Pan, H. Qing, Y. and Pei-yong, L. Direct and Indirect Measurement of Soil Suction in the Laboratory. **Electronic Journal of Geotechnical Engineering** 15 (2011): 1-14.
- Phien-wej, N., Pientong, T., Balasubramaniam, A.S. Collapse and strength characteristics of Loess in Thailand. **Engineering Geology** 32 (1992): 59-72.
- Punrattanasin, P., Subjarassang, A., Kusakabe, O., and Nishimura, T. Soil water characteristic curve for Khon Kaen loess. **Proceedings of the 8th National Convention on Civil Engineering**, GTE452-GTE457. Khon Kaen, Thailand, 2002.
- Punrattanasin, P., Subjarassang, A., Kusakabe, O., and Nishimura, T. Engineering properties of Khon Kaen loess under unsaturated condition. **Proceedings of the 8th National Convention on Civil Engineering**, GTE316-GTE321. Khon Kaen, Thailand, 2002.

- Rouf M.A., Hamamoto S., Kawamoto K., Sakaki T., Komatsu T., and Moldrup P. Unified measurement system with suction control for measuring hysteresis in soil-gas transport parameters. **Water Resources Research** (2012): 48.
- Schnellmann, R., Rahardjo, H. and Schneider, H.R. Unsaturated shear strength of a silty sand. **Engineering Geology** 162 (2013) 88-96.
- Vanapalli, S.K., Fredlund, D.G., Pufahl, D.E., and Clifton, A. Model for the prediction of shear strength with respect to soil suction. **Canadian Geotechnical Journal** 33 (1996): 379 – 392.
- Wykeham Farrance Ltd., Soil Mechanics division of Controls Group. Unsaturated Testing in the Autotriax System, PowerPoint **presentation**, 2010.
- Zhai Q., Rahardjo H. Determination of soil–water characteristic curve variables. **Computers and Geotechnics** 42 (2012): 37–43.

APPENDIX

$f_{0.05, \nu_1, \nu_2}$

		Degrees of freedom for the numerator (ν_1)																		
$\nu_1 \backslash \nu_2$		1	2	3	4	5	6	7	8	9	10	12	15	20	24	30	40	60	120	∞
		Degrees of freedom for the denominator (ν_2)	1	161.4	199.5	215.7	224.6	230.2	234.0	236.8	238.9	240.5	241.9	243.9	245.9	248.0	249.1	250.1	251.1	252.2
	2	18.51	19.00	19.16	19.25	19.30	19.33	19.35	19.37	19.38	19.40	19.41	19.43	19.45	19.45	19.46	19.47	19.48	19.49	19.50
	3	10.13	9.55	9.28	9.12	9.01	8.94	8.89	8.85	8.81	8.79	8.74	8.70	8.66	8.64	8.62	8.59	8.57	8.55	8.53
	4	7.71	6.94	6.59	6.39	6.26	6.16	6.09	6.04	6.00	5.96	5.91	5.86	5.80	5.77	5.75	5.72	5.69	5.66	5.63
	5	6.61	5.79	5.41	5.19	5.05	4.95	4.88	4.82	4.77	4.74	4.68	4.62	4.56	4.53	4.50	4.46	4.43	4.40	4.36
	6	5.99	5.14	4.76	4.53	4.39	4.28	4.21	4.15	4.10	4.06	4.00	3.94	3.87	3.84	3.81	3.77	3.74	3.70	3.67
	7	5.59	4.74	4.35	4.12	3.97	3.87	3.79	3.73	3.68	3.64	3.57	3.51	3.44	3.41	3.38	3.34	3.30	3.27	3.23
	8	5.32	4.46	4.07	3.84	3.69	3.58	3.50	3.44	3.39	3.35	3.28	3.22	3.15	3.12	3.08	3.04	3.01	2.97	2.93
	9	5.12	4.26	3.86	3.63	3.48	3.37	3.29	3.23	3.18	3.14	3.07	3.01	2.94	2.90	2.86	2.83	2.79	2.75	2.71
	10	4.96	4.10	3.71	3.48	3.33	3.22	3.14	3.07	3.02	2.98	2.91	2.85	2.77	2.74	2.70	2.66	2.62	2.58	2.54
	11	4.84	3.98	3.59	3.36	3.20	3.09	3.01	2.95	2.90	2.85	2.79	2.72	2.65	2.61	2.57	2.53	2.49	2.45	2.40
	12	4.75	3.89	3.49	3.26	3.11	3.00	2.91	2.85	2.80	2.75	2.69	2.62	2.54	2.51	2.47	2.43	2.38	2.34	2.30
	13	4.67	3.81	3.41	3.18	3.03	2.92	2.83	2.77	2.71	2.67	2.60	2.53	2.46	2.42	2.38	2.34	2.30	2.25	2.21
	14	4.60	3.74	3.34	3.11	2.96	2.85	2.76	2.70	2.65	2.60	2.53	2.46	2.39	2.35	2.31	2.27	2.22	2.18	2.13
	15	4.54	3.68	3.29	3.06	2.90	2.79	2.71	2.64	2.59	2.54	2.48	2.40	2.33	2.29	2.25	2.20	2.16	2.11	2.07
	20	4.35	3.49	3.10	2.87	2.71	2.60	2.51	2.45	2.39	2.35	2.28	2.20	2.12	2.08	2.04	1.99	1.95	1.90	1.84
	21	4.32	3.47	3.07	2.84	2.68	2.57	2.49	2.42	2.37	2.32	2.25	2.18	2.10	2.05	2.01	1.96	1.92	1.87	1.81
	22	4.30	3.44	3.05	2.82	2.66	2.55	2.46	2.40	2.34	2.30	2.23	2.15	2.07	2.03	1.98	1.94	1.89	1.84	1.78
	23	4.28	3.42	3.03	2.80	2.64	2.53	2.44	2.37	2.32	2.27	2.20	2.13	2.05	2.01	1.96	1.91	1.86	1.81	1.76
	24	4.26	3.40	3.01	2.78	2.62	2.51	2.42	2.36	2.30	2.25	2.18	2.11	2.03	1.98	1.94	1.89	1.84	1.79	1.73
	25	4.24	3.39	2.99	2.76	2.60	2.49	2.40	2.34	2.28	2.24	2.16	2.09	2.01	1.96	1.92	1.87	1.82	1.77	1.71
	26	4.23	3.37	2.98	2.74	2.59	2.47	2.39	2.32	2.27	2.22	2.15	2.07	1.99	1.95	1.90	1.85	1.80	1.75	1.69
	27	4.21	3.35	2.96	2.73	2.57	2.46	2.37	2.31	2.25	2.20	2.13	2.06	1.97	1.93	1.88	1.84	1.79	1.73	1.67
	28	4.20	3.34	2.95	2.71	2.56	2.45	2.36	2.29	2.24	2.19	2.12	2.04	1.96	1.91	1.87	1.82	1.77	1.71	1.65
	29	4.18	3.33	2.93	2.70	2.55	2.43	2.35	2.28	2.22	2.18	2.10	2.03	1.94	1.90	1.85	1.81	1.75	1.70	1.64
	30	4.17	3.32	2.92	2.69	2.53	2.42	2.33	2.27	2.21	2.16	2.09	2.01	1.93	1.89	1.84	1.79	1.74	1.68	1.62
	40	4.08	3.23	2.84	2.61	2.45	2.34	2.25	2.18	2.12	2.08	2.00	1.92	1.84	1.79	1.74	1.69	1.64	1.58	1.51
	60	4.00	3.15	2.76	2.53	2.37	2.25	2.17	2.10	2.04	1.99	1.92	1.84	1.75	1.70	1.65	1.59	1.53	1.47	1.39

BIOGRAPHY

Name:	Miss Maria Emilia Pambid Sevilla		
Date of Birth:	April 5, 1987		
Telephone:	Mobile +66889024311		
E-mail:	sevilla_emilia@yahoo.com		
Education:	<u>Year</u>	<u>Institute</u>	<u>Degree</u>
	2010	De La Salle University	Bachelor of Science in Civil Engineering with Specialization in Hydraulics and Water Resources

Awards and Scholarships

AUN-Seed Net Masteral Degree Scholarship Program, 2011.

Honorable Mention, De La Salle University, 2010.

Most Outstanding Civil Engineering Student, De La Salle University, 2010.

Nominated, Achiever Scholar Program, De La Salle University, 2010.

Publications

Likitlersuang, S. and Sevilla, M. E. P. 2013. Parametric Study of Soil-Water Curves of Sands. 5th AUN/SEED-Net Regional Conference in Geological Engineering. Kuala Lumpur, Malaysia.

Sevilla, M. E. P., and Likitlersuang, S. 2013. Soil-Water Characteristic Curve of Compacted Toyoura Sand with Varying Degrees of Constant Pore Water Pressures. 18th National Convention on Civil Engineering. Chiang Mai, Thailand.

Terante, D.C., Lamberte, A.E. and Sevilla, M. E. P. 2010. Risk-based Analysis of a Flood Plain: A Case in the City of Malabon. 5th Civil Engineering Conference in the Asian Region and Australasian Structural Engineering Conference. Sydney, Australia. 859-867.